2016年1月19日　第２回サーフスワークショップ@筑波大学

物質変換材料部門の成果報告

筑波大学　数理物質系　中村潤児

講演内容

- 物質変換材料部門の研究内容
- 主な研究成果
- 具体例：CO_2活性化におけるEley-Rideal型メカニズムの発見
- 具体例：燃料電池における白金触媒量の削減

物質変換材料研究部門
触媒学理に基づく環境エネルギー材料の創成

PI：中村潤児　　共同研究者：神原教授、山本准教授、近藤准教授
他連携研究員14名

二酸化炭素のメタノールへの転換

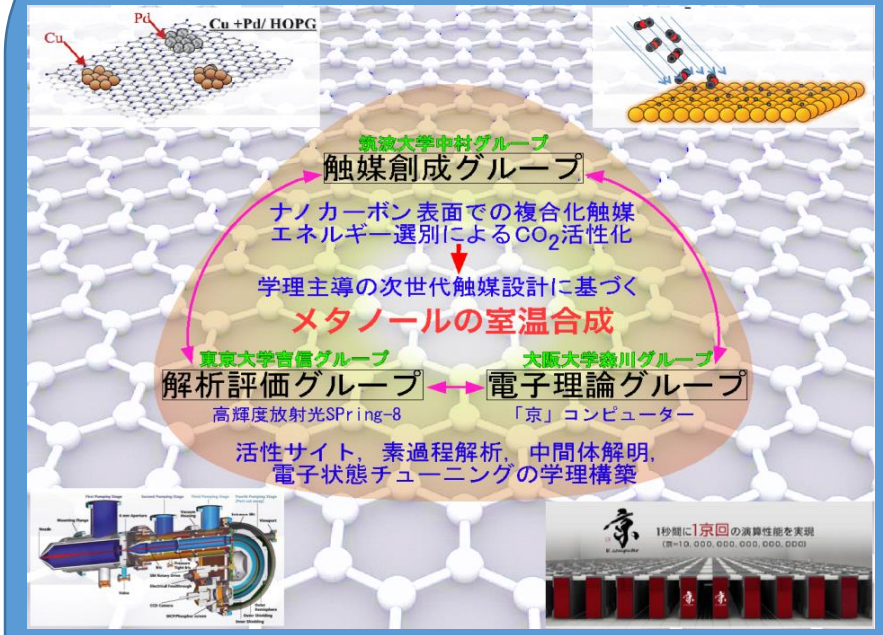

JST　ACT-Cプロジェクト進行中 平成24～29年

排ガス中のCO_2を化学的に転換する
最有力手法

白金を代替する燃料電池触媒

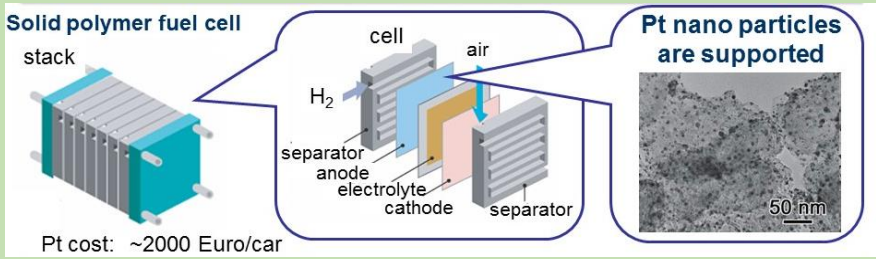

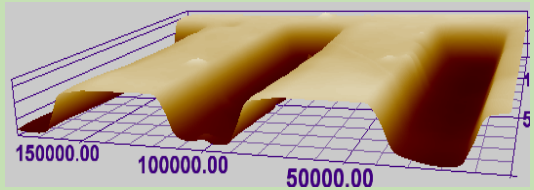

カーボン触媒で国際的にリード
Nano Lett (2009)は618回引用、
Nature Comm.(2012), Sci.Rep.(2014),
Sci.Rep.(2015), Science (2016)

燃料電池の普及に貢献

物質変換材料部門の研究内容

1. CO_2 のメタノールへの転換

CO_2活性化機構解明、グラフェン触媒の応用、計算科学(阪大)と放射光実験(物性研)の共同研究

2. 燃料電池用カーボン触媒の開発

炭素/白金界面相互作用の解明、カーボンアロイ触媒の機能と設計

3. 触媒機能の学理構築

グラファイト系炭素の酸塩基性の起源、担体効果の解明、物性物理と反応性の橋渡し

4. 藻類産生油の触媒的転換

C_{30} - C_{40}化学の構築、クラッキング、異性化、重合、ハイブリッド化

5. 光デバイスのための材料合成

ポリマーやグラフェンを用いた発光・レーザー、太陽電池材料

6. 新分光法と新物質

ヘテロダイン分光法のSTSへの応用、新二次元物質の創出

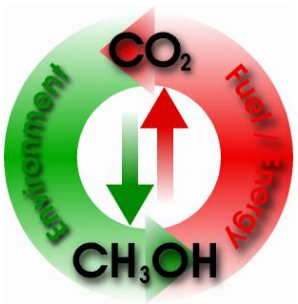

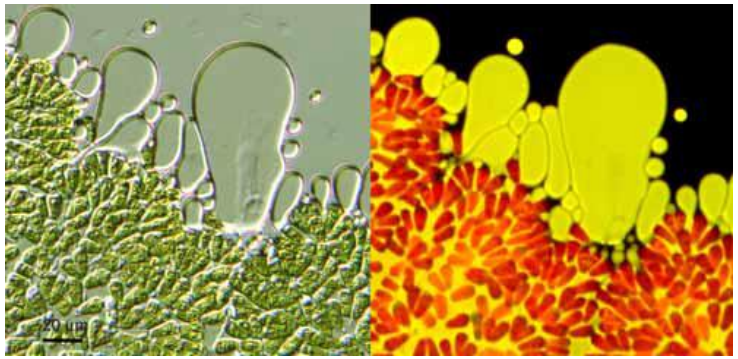

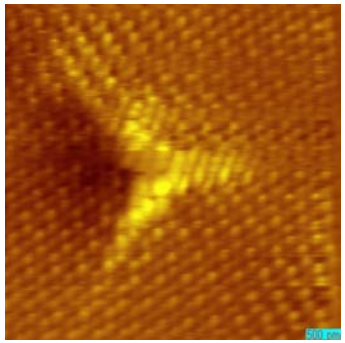

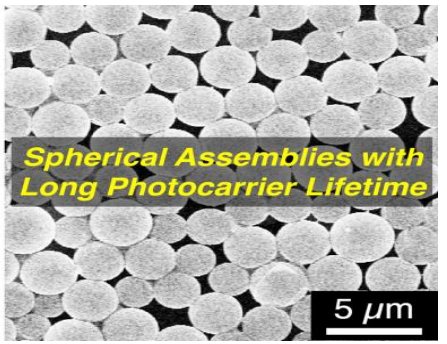

主な研究業績

1. 受賞

・2014年4月　文部科学大臣表彰　若手科学者賞　山本
・2014年6月　筑波大学若手教員特別奨励賞　山本
・2015年9月　高分子学会日立化成賞　山本
・2015年11月　BCSJ賞　（日本化学会）　神原・桑原ら
・2016年3月　日本物理学会若手奨励賞　（日本物理学会）　近藤

2. 大型研究費

・平成25–28年度　研究費 若手研究A　山本（2,457万円）
・平成22–26年度 固体高分子形燃料電池実用化推進技術開発/基盤技術開発/カーボンアロイ触媒　近藤（8,415万円）
・平成24–27年度　JSTさきがけ　近藤（5,200万円）
・平成24–29年度　JST ACT-C　中村（11,658万円）
・平成27–28年度　公益信託ENEOS水素基金　第3分野＜CO_2固定化技術＞　近藤（1,000万円）

3. 主な論文 (2014-2015　Science, Nature系　ジャーナル5件）

・Takaki Kanbara *et al.*, "Effects of the Terminal Structure, Purity, and Molecular Weight of an Amorphous Conjugated Polymer on Its Photovoltaic Characteristics", *ACS Appl. Mater. Interfaces*, ASAP, 2016.
・Takaki Kanbara, Yohei Yamamoto *et al.*, "Self-assembled conjugated polymer spheres as fluorescent microresonators" **Sci. Rep.**, **4**, 5902/1–5, 2014.
・Takaki Kanbara, Yohei Yamamoto *et al.*, "Optically induced mode splitting in self-assembled, high quality-factor conjugated polymer microcavities" **Sci. Rep**., in press.
・Takahiro Kondo, Junji Nakamura *et al.*, "Principles and Application of Heterodyne Scanning Tunnelling Spectroscopy" **Sci. Rep.**, **4**, 6711-1～6711-5, 2014.
・Takahiro Kondo, Junji Nakamura *et al.*, "Observation of Landau levels on nitrogen-doped flat graphite surfaces without external magnetic fields" **Sci. Rep.**, **5**, 16412-1～16412-8, 2015.
・Takahiro Kondo, Junji Nakamura *et al.*, " Active sites of nitrogen-doped carbon materials for oxygen reduction reaction clarified using model catalysts" **Science**, 2016 in press
・Takaki Kanbara *et al.*, "Direct Arylation Polycondensation: A Promising Method for the Synthesis of Highly Pure, High-Molecular-Weight Conjugated Polymers Needed for Improving the Performance of Organic Photovoltaics" *Adv. Funct. Mater.*, **24**, 3226-3233, 2014.

4. その他

・特許申請8件、学生・ポスドクの受賞24件（2014-2015年度）　　Science誌論文に関する記者発表　2016年1月21日

Eley-Rideal Type Mechanism of Formate Synthesis by hydrogenation of Carbon Dioxide on Cu Surfaces

Jiamei Quan, Tetsuya Ogawa, Takahiro Kondo, Guichang Wang, Junji Nakamura

Ph.D. student Jiamei Quan

Submitted

Acknow¥edgment$

JST ACT-C 先導的物質変換領域

$(\Theta_{Zn} \geqq 0.3)$

The most promising catalytic conversion of CO_2 : CH_3OH synthesis

CO_2 + H_2

formate ⇄ methoxy ⇄ methanol

Cu(111)

$CO_2 + 3H_2 \rightarrow CH_3OH + H_2O$

250˚C, 5 MPa

house... als... ΔH= -49.4 kJ/mol

Low temp is favored because of high equilibrium yield

formate → methoxy ← methanol

Zn/Cu(111)

(Ohnishi 1988)

Formate synthesis is the initial step of CO_2 hydrogenation

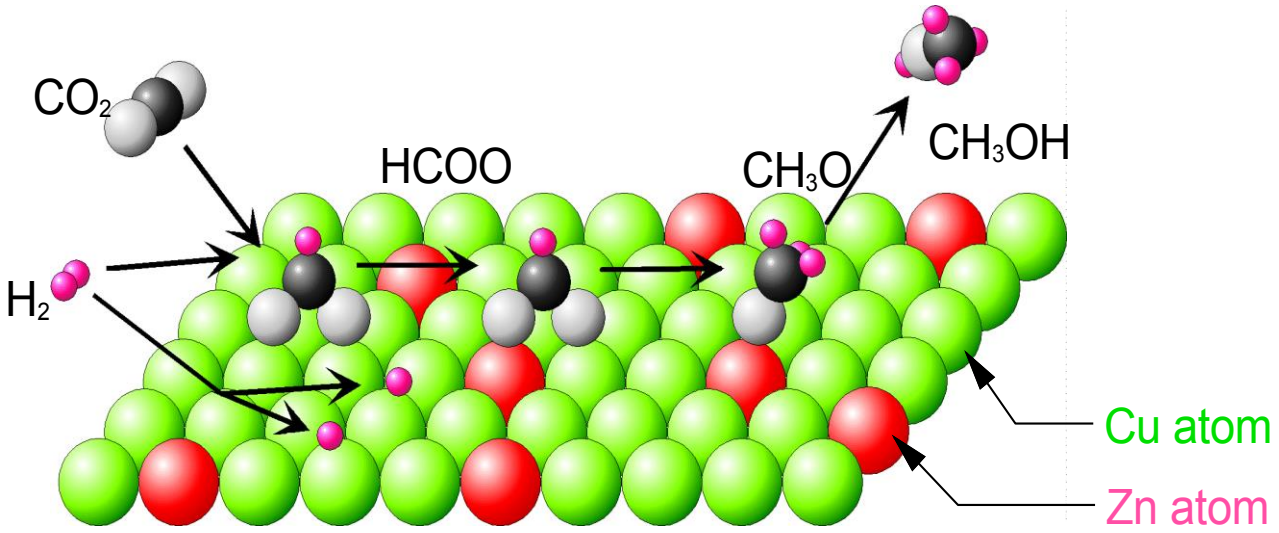

Surface inermediates

$$H_2 + CO_2 \Leftrightarrow \underset{\text{(Formate)}}{HCOO_a} \Leftrightarrow \underset{\text{(Methoxy)}}{CH_3O_a} \Leftrightarrow \underset{\text{(Methanol)}}{CH_3OH}$$

at Cu-Zn site

J. Nakamura, et al., *Topics in Catalysis*, **22** (2003) 277.

Suggestions for Eley-Rideal (E-R) type mechanism

High pressure kinetic measurements (760 Torr)

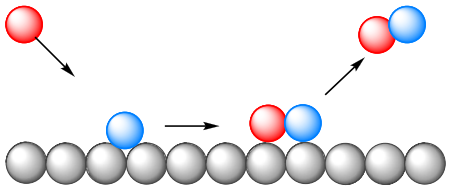

H. Nakano, J. Nakamura, J. Phys. Chem. B 2001, 105, 1355

1) Formate synthesis reaction rate

$$R \propto \frac{P_{H_2}^{1/2} P_{CO_2}}{(1+kP_{H_2}^{1/2})^1}$$

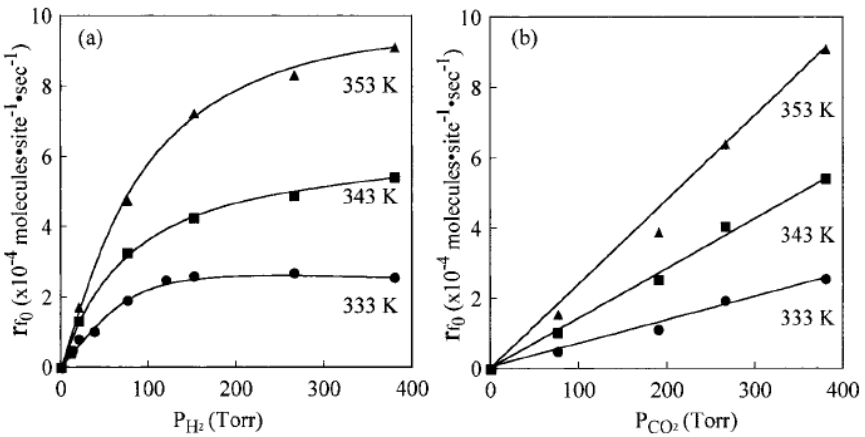

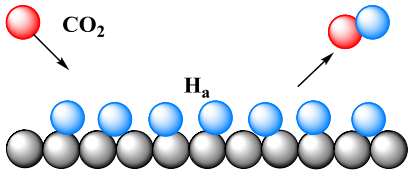

H_a does not hinder CO_2 adsorption

2) Surface structure insensitivity

The activation energy of

Cu(110): 59.8 ± 4.1 kJ mol^{-1};

Cu(100): 55.6 ± 8.0 kJ mol^{-1};

Cu(111): 56.6 ± 5.9 kJ mol^{-1}.

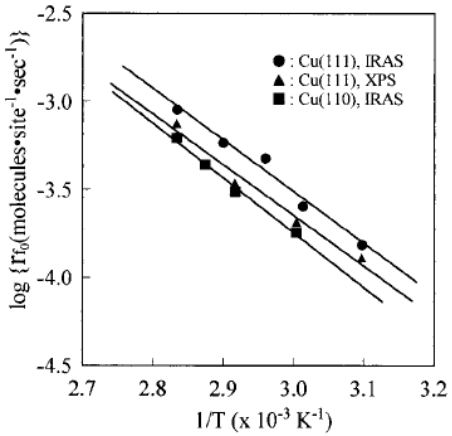

3) Organometallic chemistry

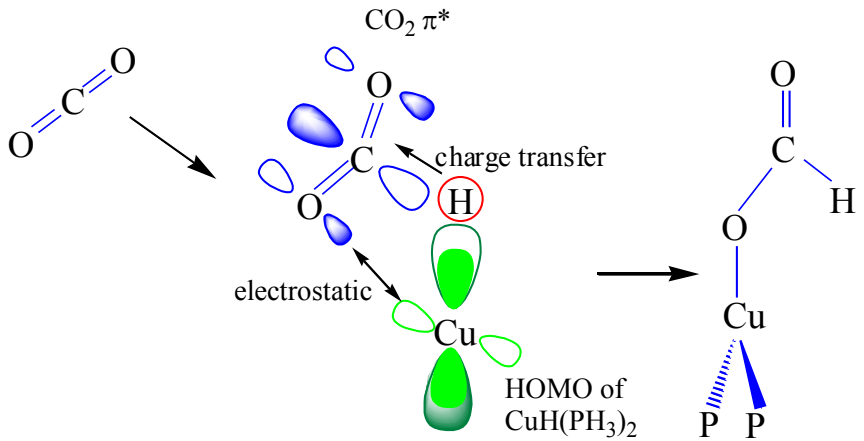

Sakaki et al. Inorg. Chem. 28(1989)2583

Objective

To prove the ER type mechanism for formate synthesis on Cu using CO_2 molecular beam

Supersonic CO_2 molecular beam

UHV

Hot CO_2

$$CO_2 + H_a \rightarrow HCOO_a$$

We can realize

$T_{gas} = \nabla T_{surf}$

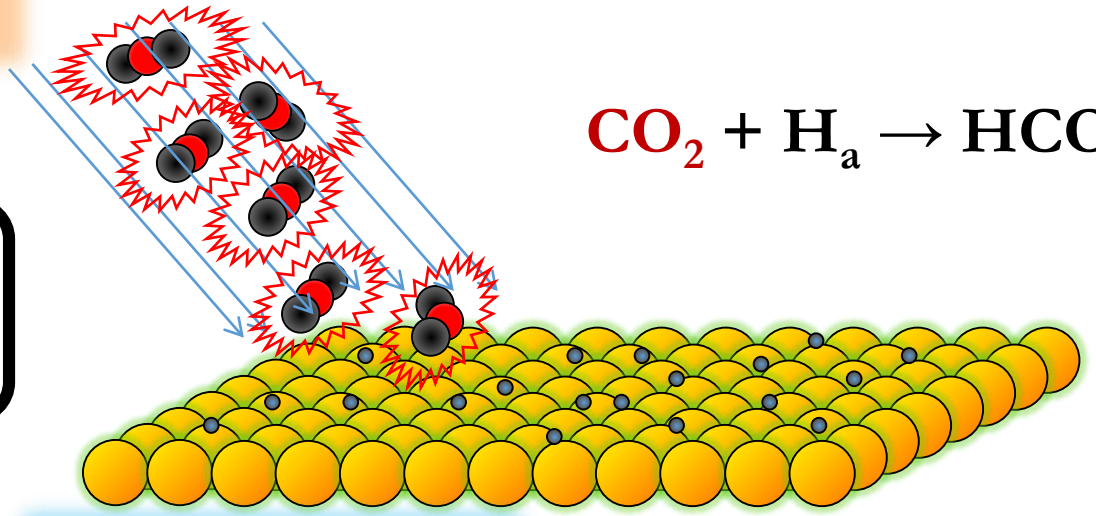

Cold Cu surface

Hydrogen covered Cu(111) or Cu(110)

Translational and vibrational energy of CO_2

（X:portion of gas、Cp: specific heat）

$$E_{calc} = \left(\frac{m_a \sum_i X_i}{\sum_i m_i X_i} \right) \int_0^{T_n} \frac{\left(\sum_i X_i C_{pi} \right)}{\left(\sum_i X_i \right)} dT$$

CO_2 in He

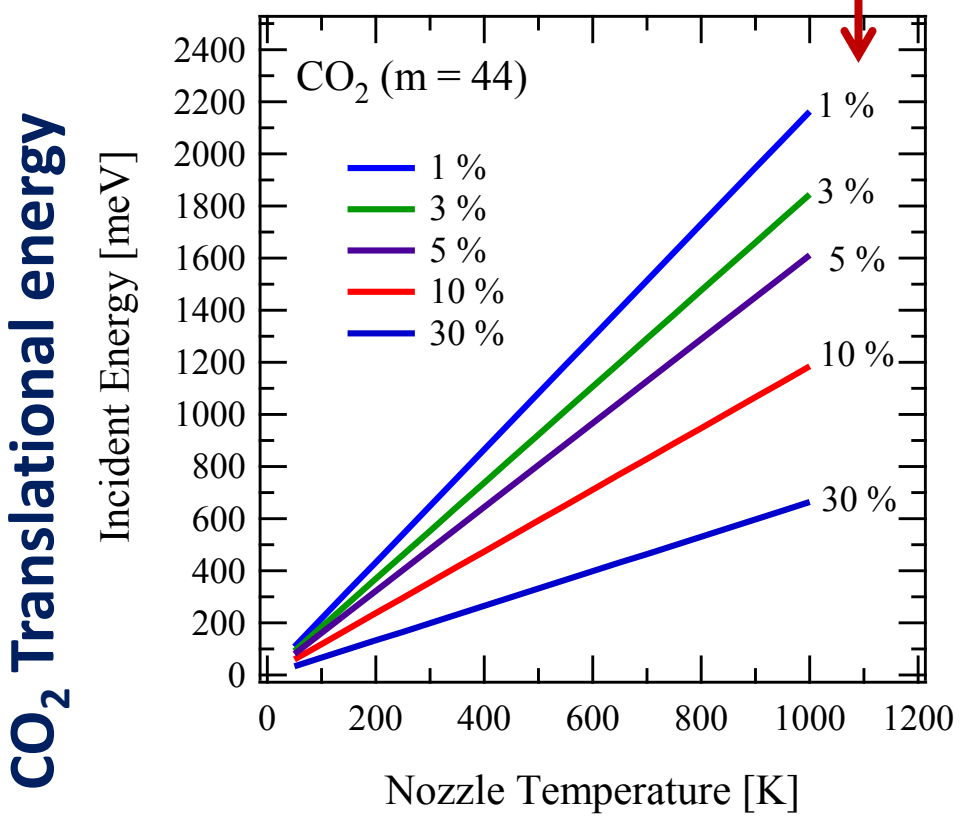

CO_2 Translational energy

We can control translational and vibrational energies of CO_2

Nozzle Temp.（= CO_2 Vibrational Temp.）

Supersonic molecular beam

Supersonic He beam

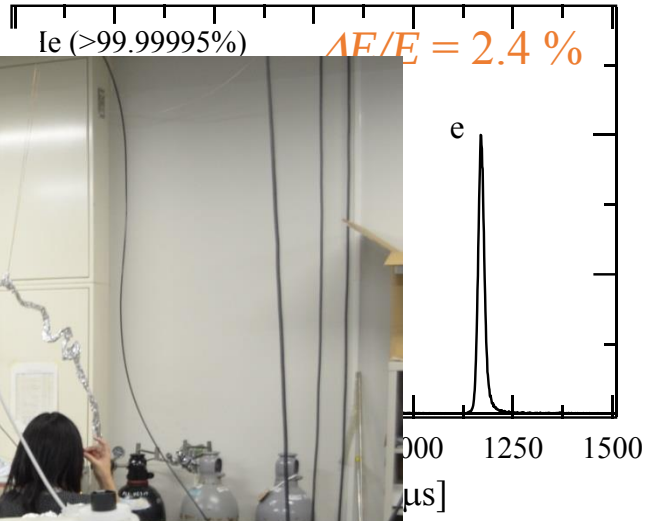

: < $3x10^{-7}$ Torr

: < $2x10^{-8}$ Torr

: < $1x10^{-10}$ Torr

Second chopper chamber: < $1x10^{-10}$ Torr

5 Detector chamber : < $9x10^{-11}$ Torr

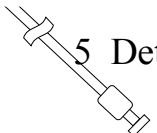

T. Kondo, *et al*. Eur. Phys. J D 38 (2006) 129.
T. Kondo et al., J. Chem. Phys. 127 (2007) 094703.

Experiments

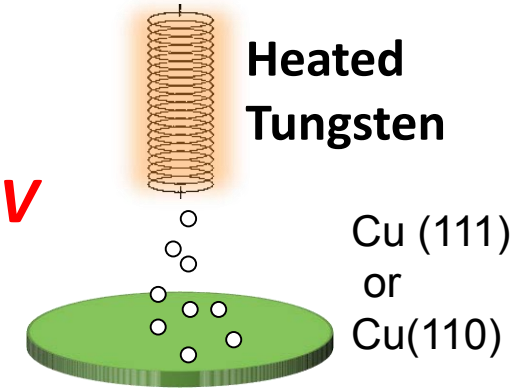

Pre-adsorption of atomic hydrogen

(200 K, 10 L) $H_2 \rightarrow 2H_a$

Supersonic CO_2 molecular beam

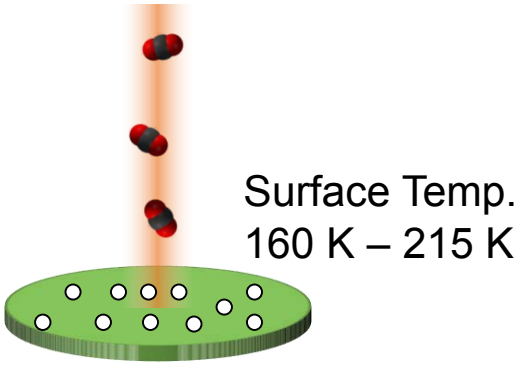

Exposure of CO_2

$H_a + CO_2 \rightarrow HCOO_a$

To examine HCOO formation

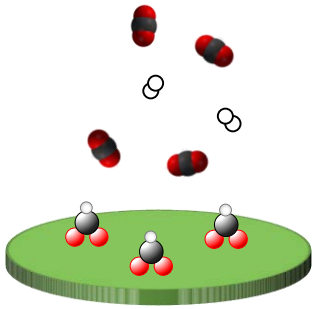

TPD (2 K/sec)

$HCOO_a \rightarrow CO_2(g) + ½\ H_2(g)$

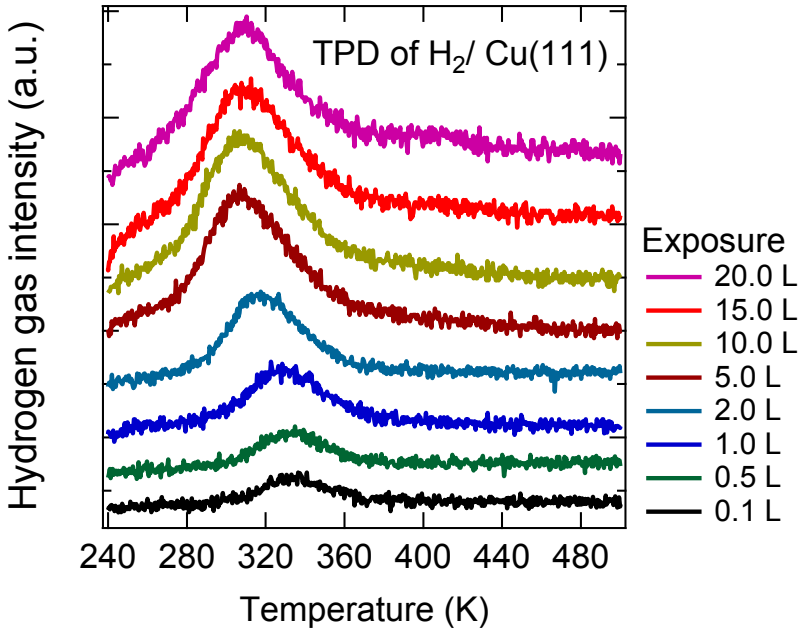

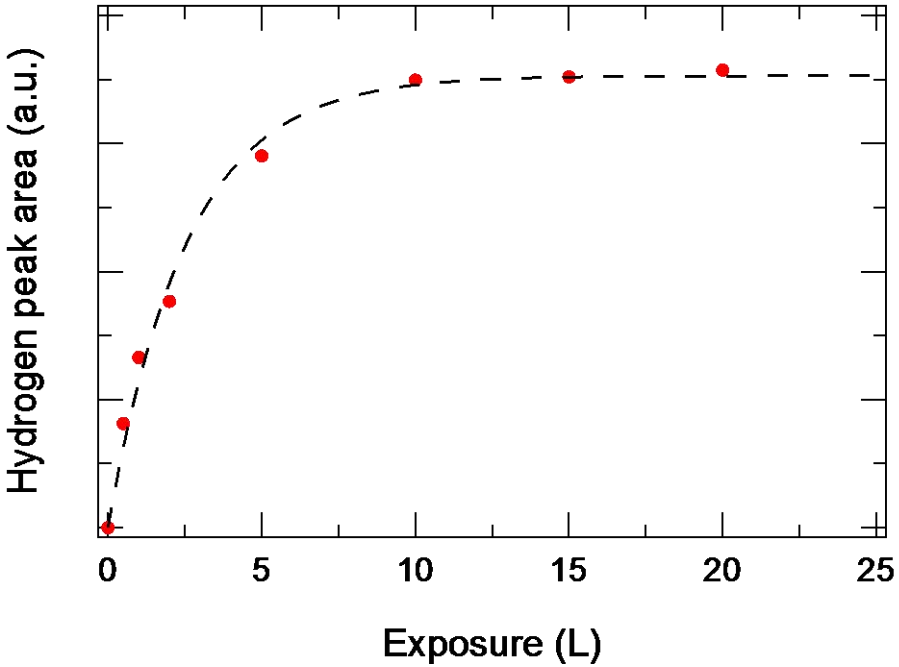

Results : TPD after 2.98×10^4 L CO_2 exposure

H/Cu(111)

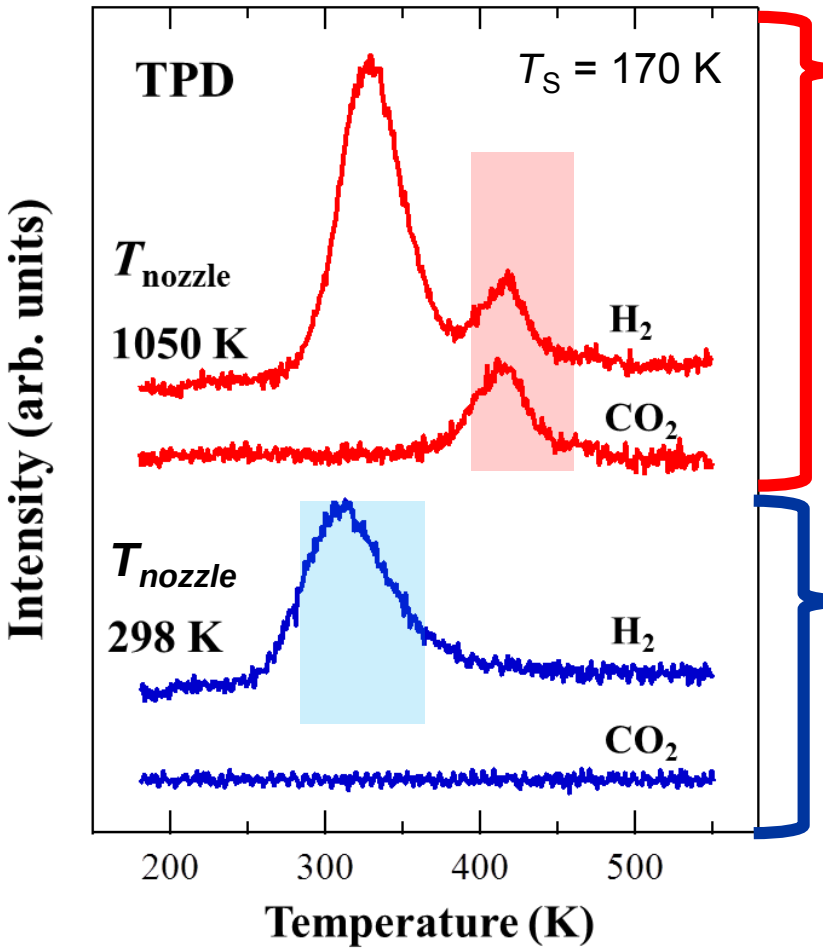

T_{nozzle} = 1050 K, E_i = 1.3 eV

410 K : Simultaneous desorption CO_2 : H_2 = 2:1

(1) The formate decomposition Temp. on Cu(111)

(2) Corresponds to the decomposition stoichiometry

$$2HCOO_a \rightarrow 2CO_2(g) + H_2(g)$$

T_{nozzle} = 298 K, E_i = 0.37 eV

310 K : Associative desorption of H_2 from Cu

$$H_a + H_a \rightarrow H_2$$

Formate is synthesized on Cu by hot CO_2 beam at T_s=170 K in UHV !

Results : Nozzle temperature dependence on Cu(110)

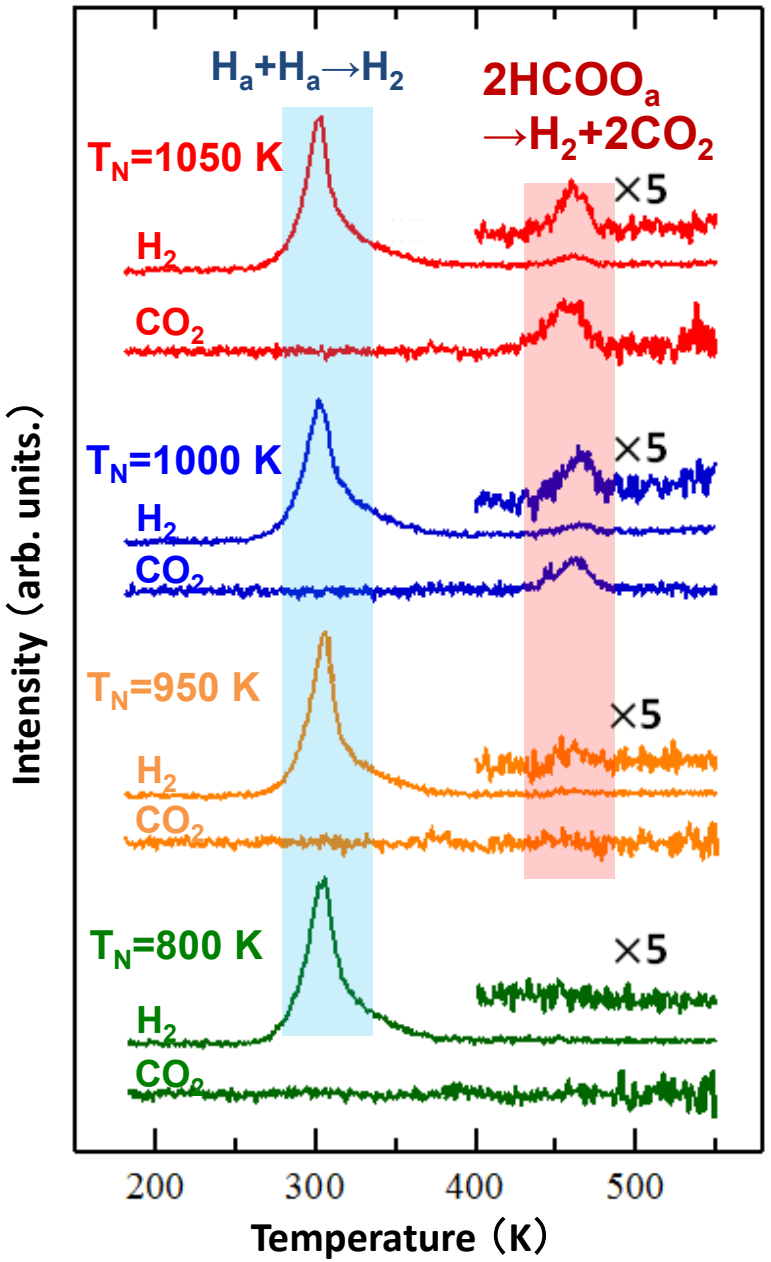

CO_2 exposure :3.36x10^4 L, T_s = 215 K

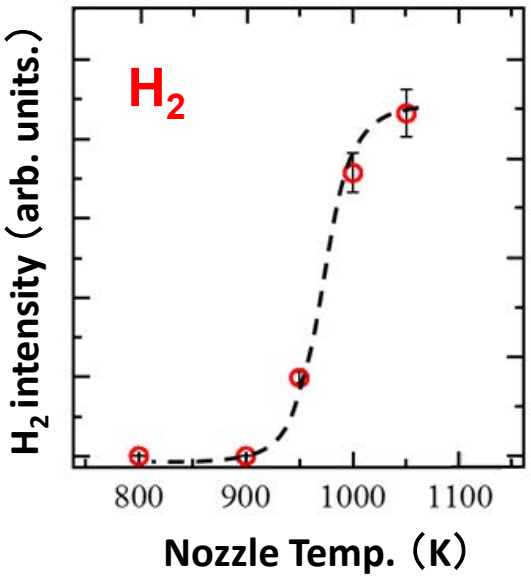

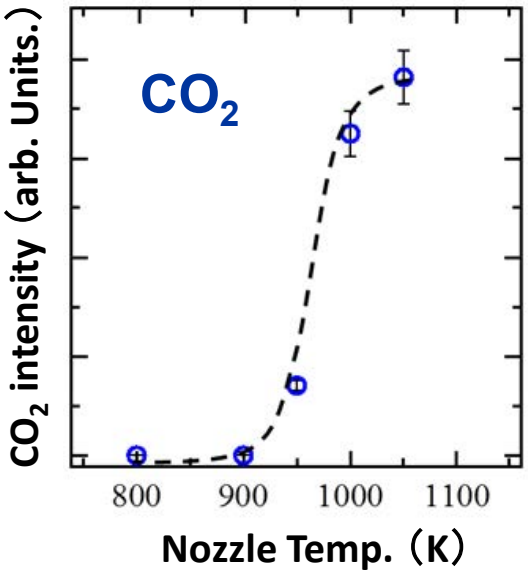

Reaction occurs at

T_n > 950 K (E_i = 1.2 eV)

Results : Surface temperature dependence on Cu(110)

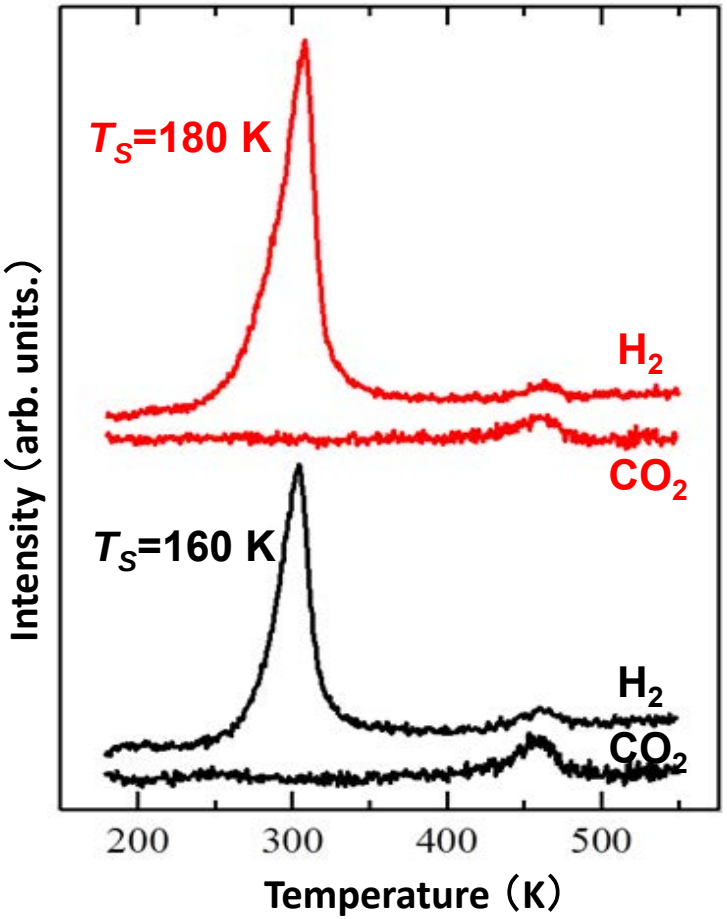

CO_2 exposure :3.36x10^4 L, T_{nozzle} = 1000 K

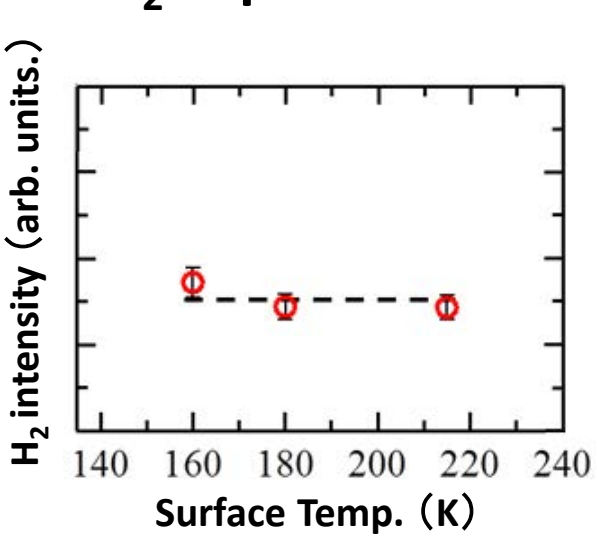

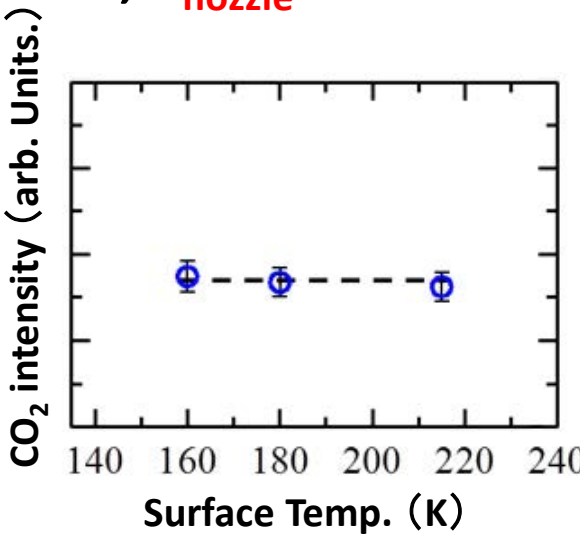

No surface temperature dependence !!

No thermal trapping
or direct reaction without precursor

Thermal non-equilibrium dynamics
and
Eley-Rideal type mechanism

Results: Reaction probability on Cu(111)

Molecular beam

CO_2 exposure : 2.75×10^4 L

T_{nozzle} = 1050 K

UHV

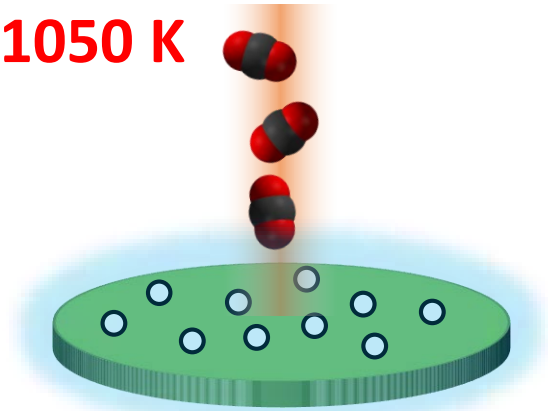

Cu(111), T_S = 170 K

Initial reaction probability of formate synthesis is derived as $p = 2.2 \times 10^{-4}$

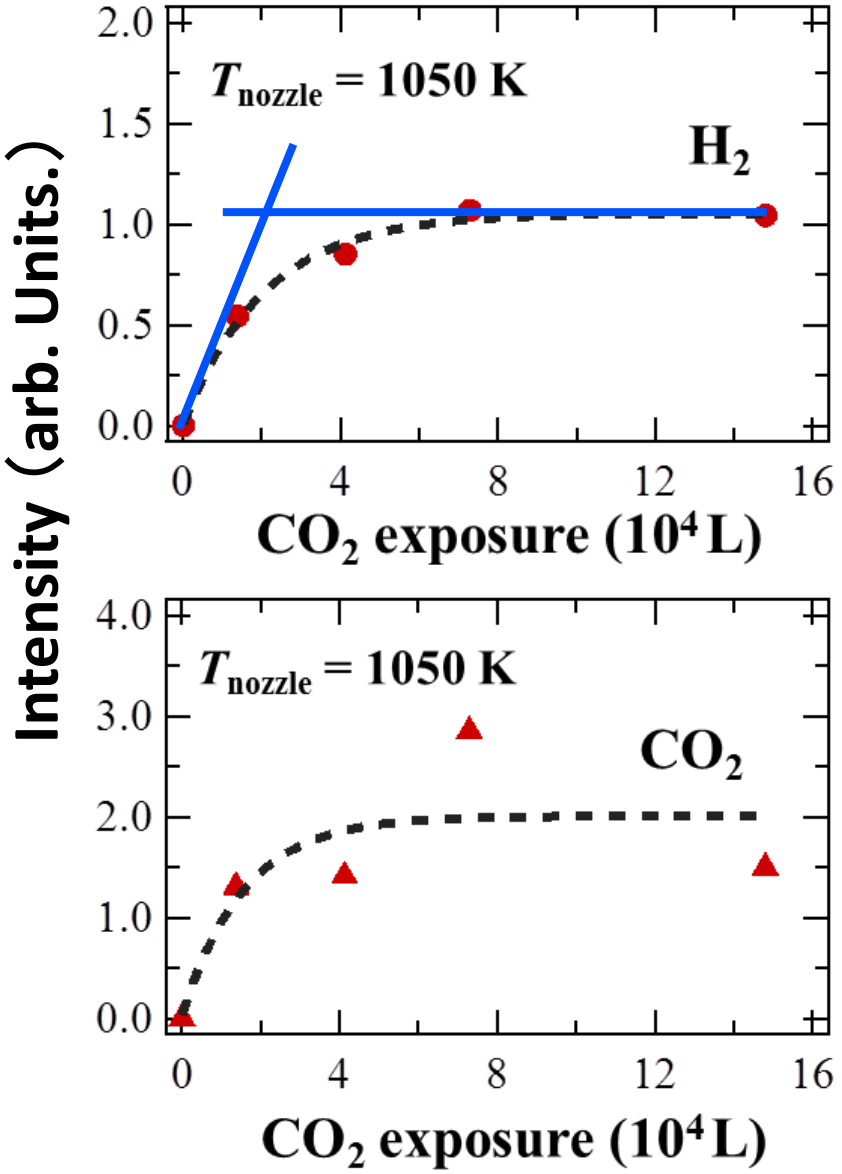

Results: Reaction probability on Cu(111)

Molecular beam

CO_2 exposure : 2.75×10^4 L

T_{nozzle} = 1050 K

UHV

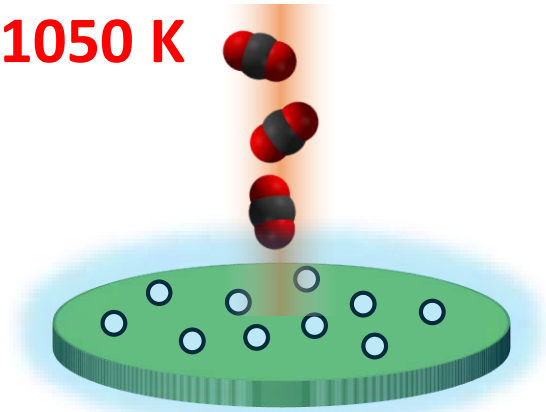

Cu(111), T_S = 170 K

High pressure cell

T_s = 350 K

T_{gas} = 350 K

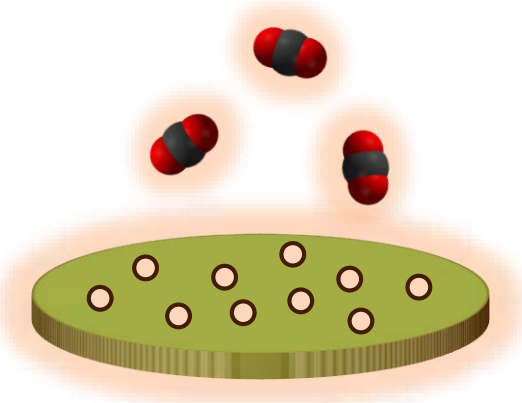

760 Torr

J. Nakamura, et al., *J. Phys. Chem. B* **2001**, 105, 1355.

Initial reaction probability of formate synthesis is derived as $p = 2.2 \times 10^{-4}$

Comparison with the high-pressure experiment

Molecular beam

CO_2 exposure : 2.75×10^4 L

T_{nozzle} = 1050 K

UHV

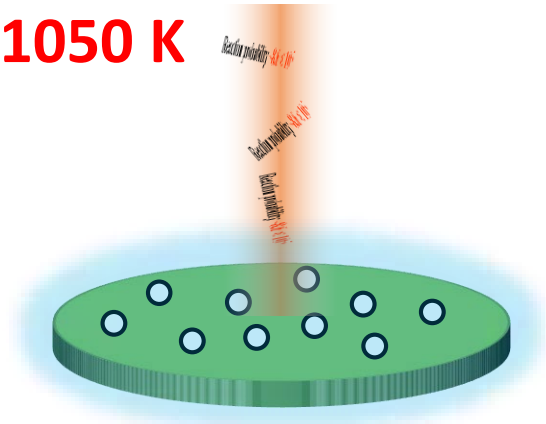

Cu(111), T_S = 170 K

Initial reaction probability of formate synthesis is derived as p = 2.2×10^{-4}

High pressure cell

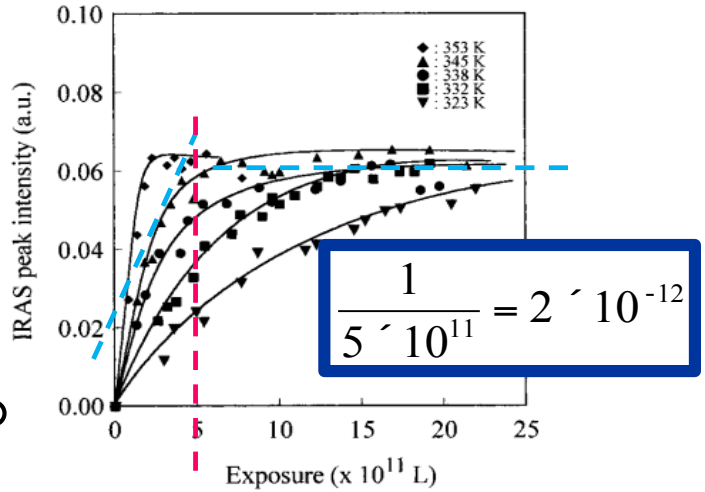

J. Nakamura, et al., *J. Phys. Chem. B* **2001**, 105, 1355.

Cu temperature ~ 350 K
CO_2 temperature ~ 350 K

Reaction probability ~ 2×10^{-12}

If we extraporate

Cu temperature ~ 1050 K
CO_2 temperature ~ 1050 K

Reaction probability ~ 8.6×10^{-7}

DFT also shows Eley-Rideal type mechanism

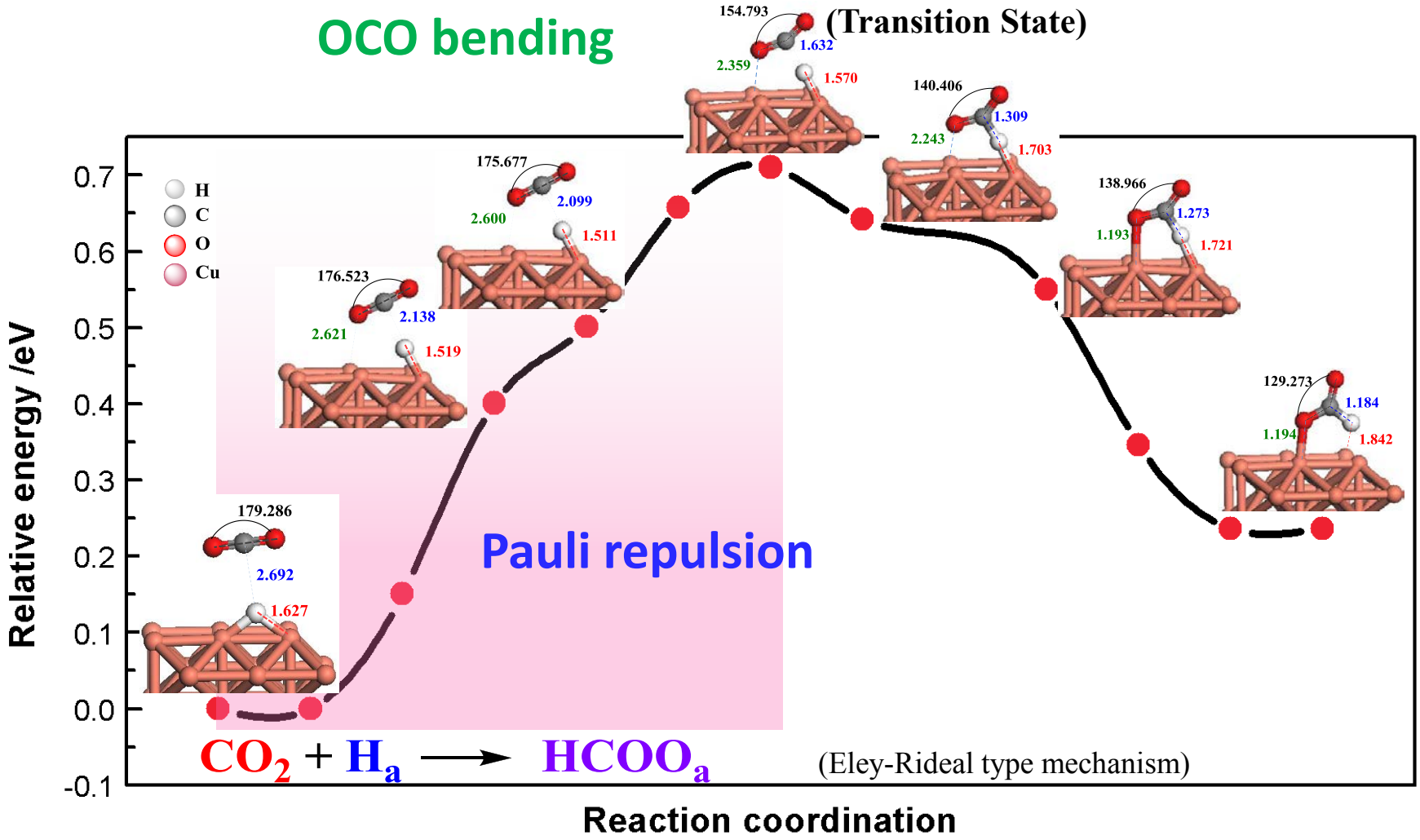

(1) CO_2 need to approach against Pauli repulsion by Cu *s* electrons

Translational energy is required

(2) OCO angle is need to bend to make sp^2-like configuration

Vibrational energy is required

Walsh diagram of CO_2

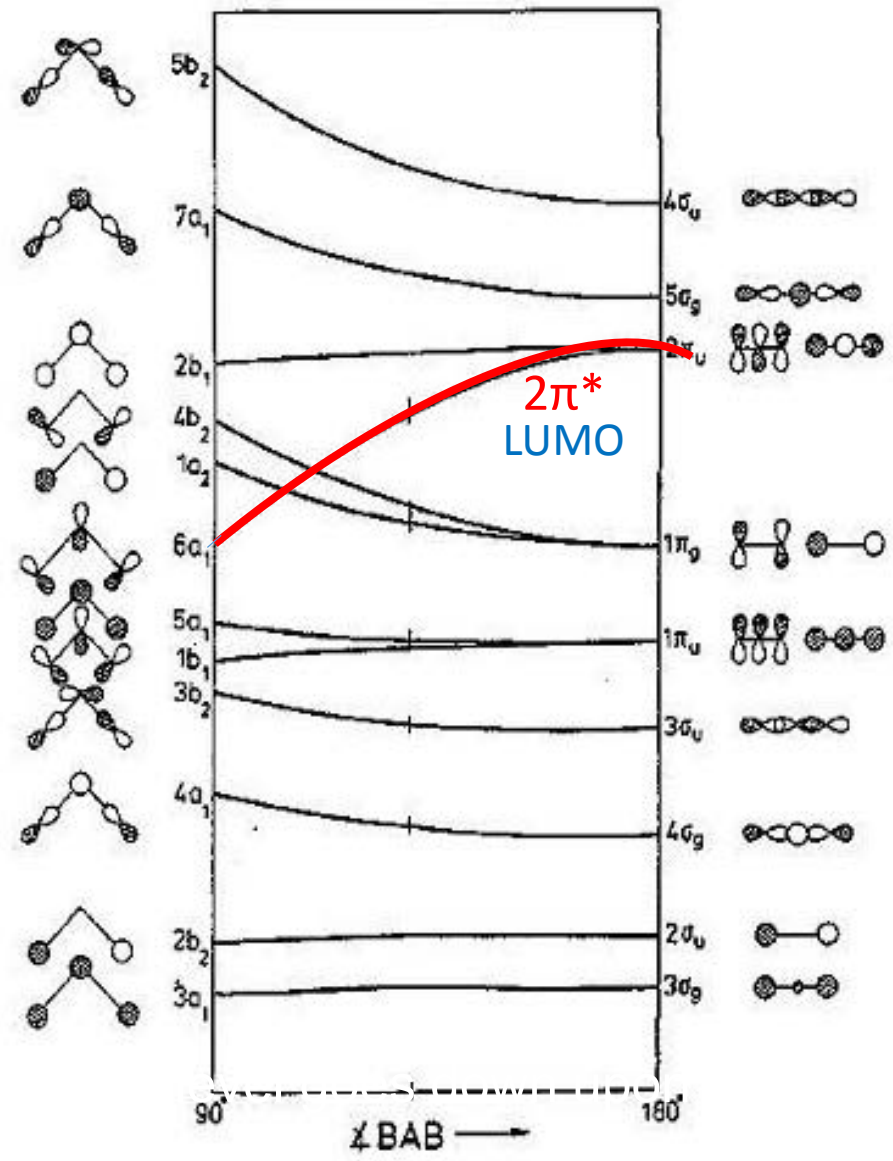

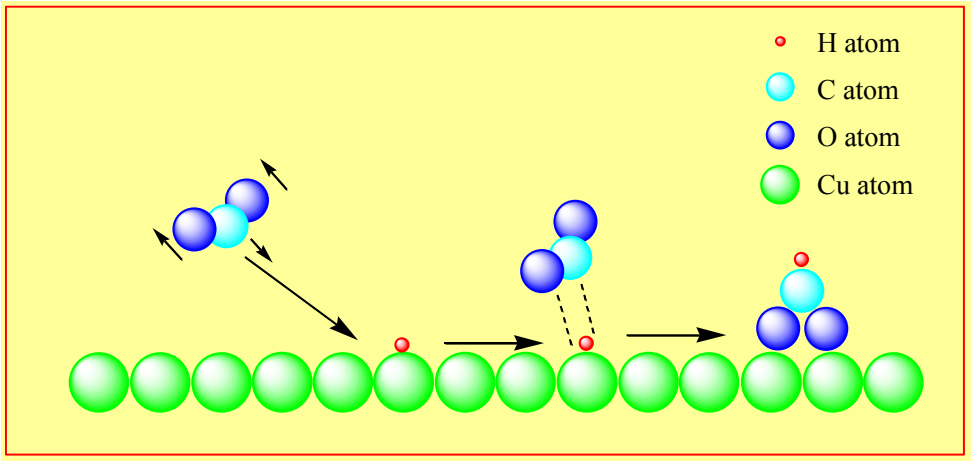

LUMO level goes down
upon bending significantly

LUMO level determines
the reactivity of acidic CO_2 molecules

Reactivity may be changed by
vibration energy of CO_2

Conclusion

Formate synthesis on Cu surfaces

$$H_2 + 2CO_2 \rightarrow 2HCOO_a$$

(1) Reaction dynamics:

Thermal non-equilibrium process

(2) Reaction mechanism:

Eley-Rideal typed mechanism

Nitrogen-doped HOPG model catalysts

Measuring catalytic activity of ORR (oxygen reduction reaction)

$$O_2 + 4\,H^+ + 4\,e^- \rightarrow 2\,H_2O$$

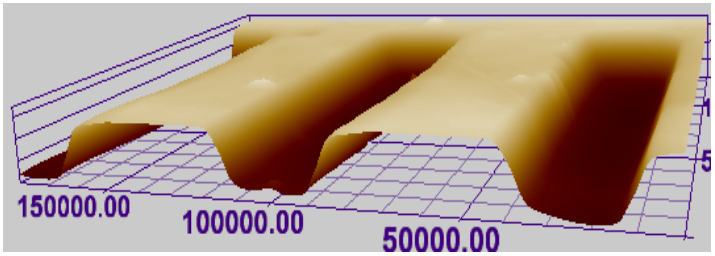

Guo, Kondo, Shibuya, Akiba, Saji, JN, *Science*, in press

The majority is graphitic nitrogen in N_2^+ bombardment

Conventional nitrogen doping method

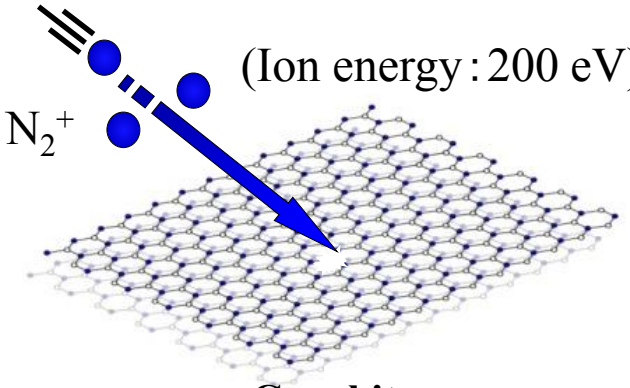

Graphitic nitrogen

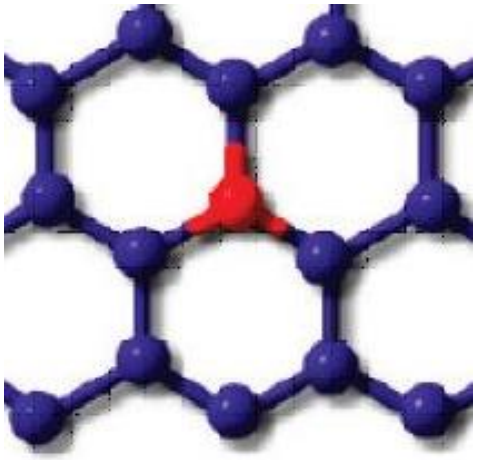

Pyridinic nitrogen

Majority (50~90 %)

Minority (10~50 %)

Difficult to prepare a pyridinic nitrogen dominant surface

Sample Preparation of N doped Graphite

Pyridinic-N dominant HOPG (*pyr*N-HOPG) preparation

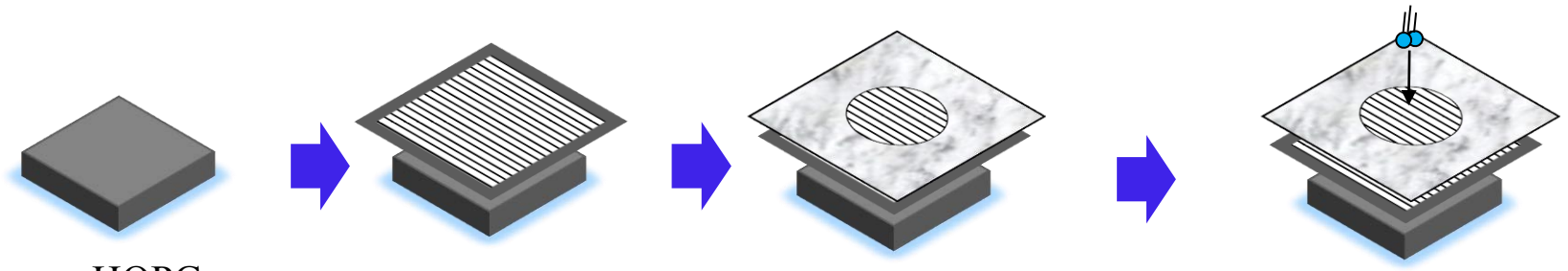

HOPG
(Highly Oriented
Pyrolytic Graphite)

Overlaying
Ni patterned mask

Overlaying
Covered mask with hole

N_2^+ bombardment
(Introducing N and edge)

Ion energy : 500 eV
N_2 pressure: 1.0 x 10^{-4} Torr

Doping pyridinic nitrogen at edges

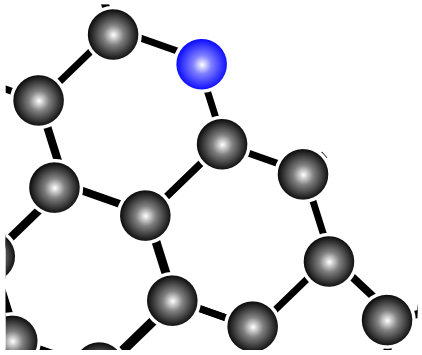

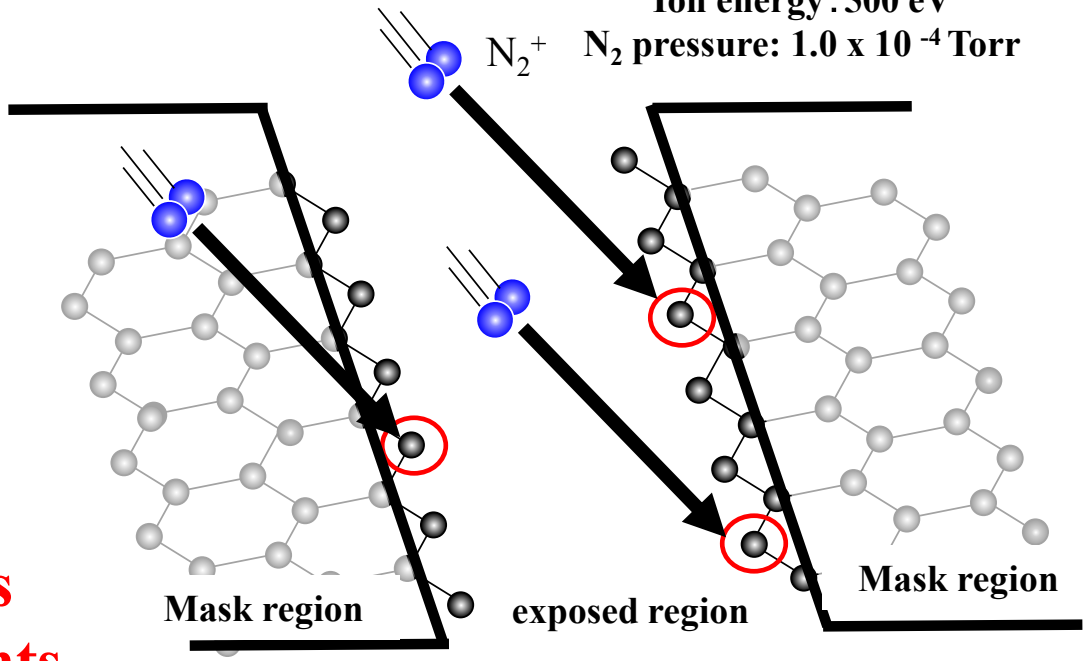

Sometimes pyridinic N is prepared by NH_3 treatments

Pyridinic nitrogen is doped at the edges of HOPG

Edges patterned HOPG

a **Optical microscopy**

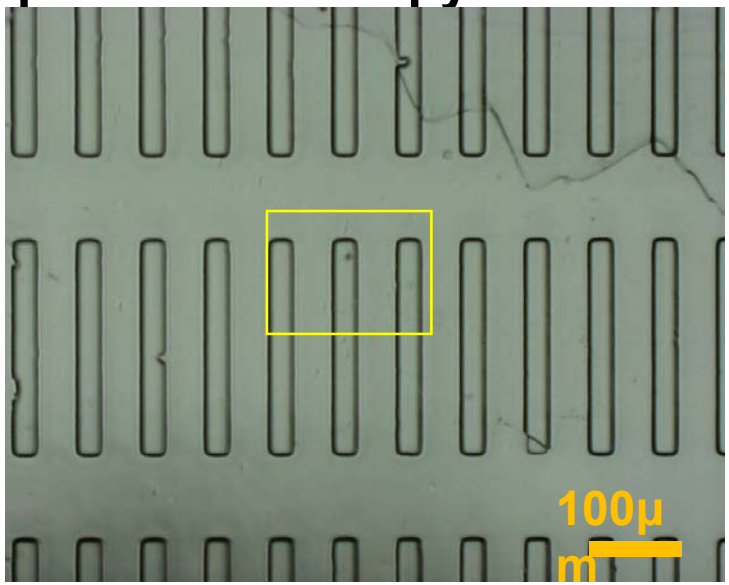

b **AFM**

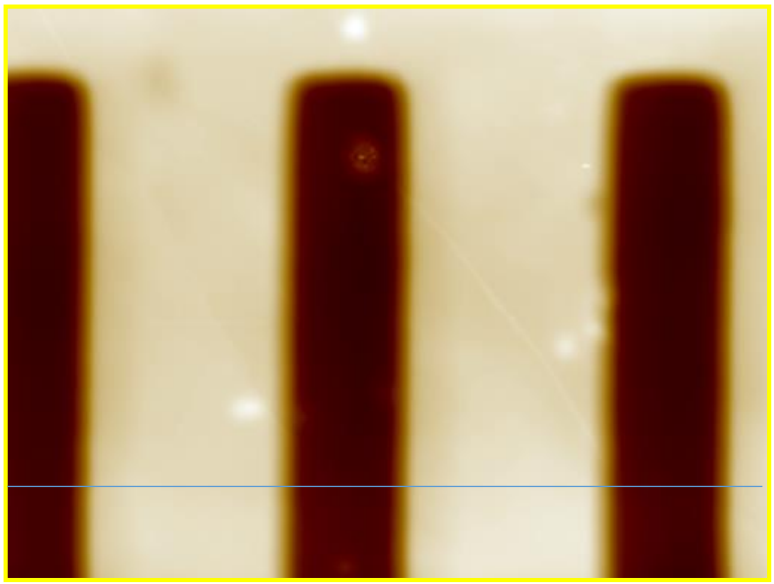

c **AFM**

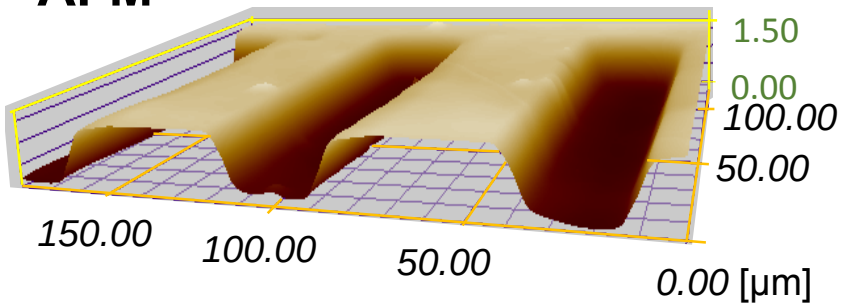

d **Line profile**

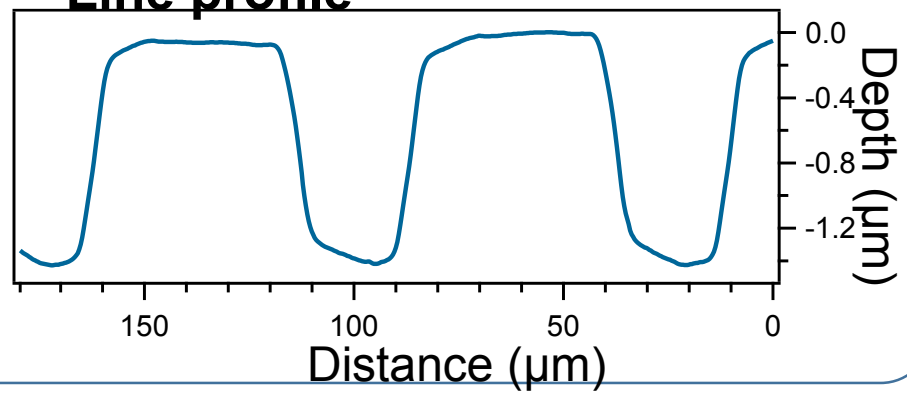

Series of HOPG model catalysts & CO_2 adsorption

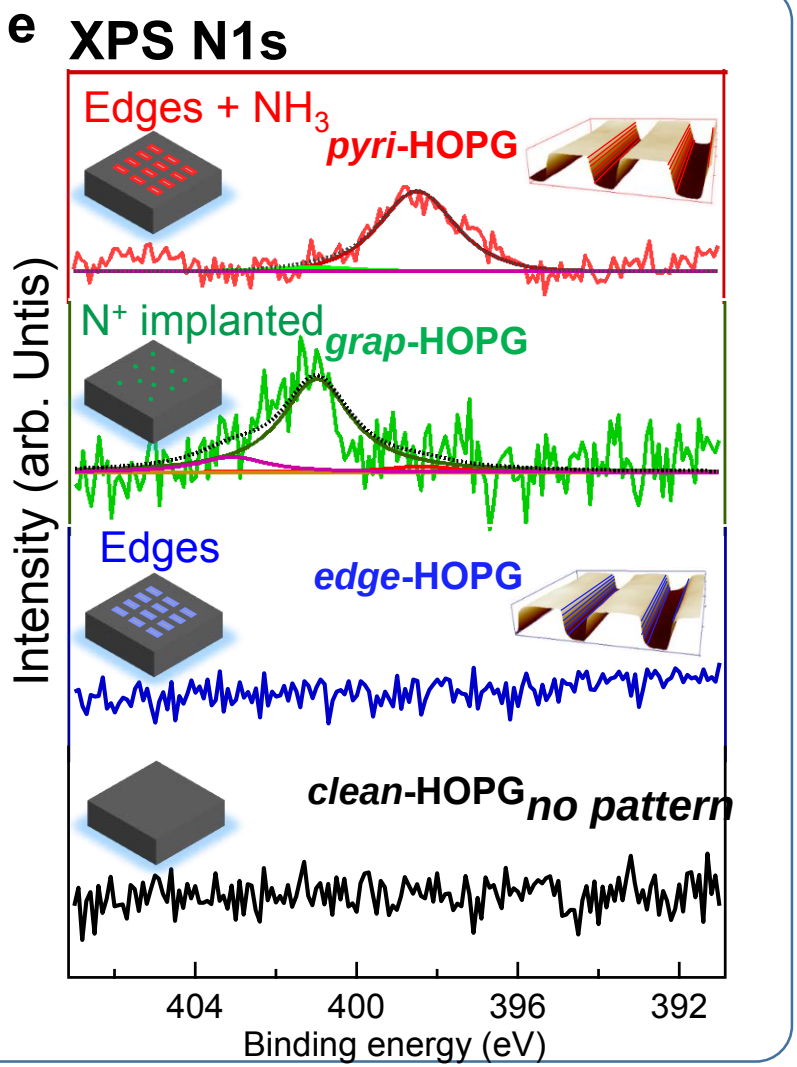

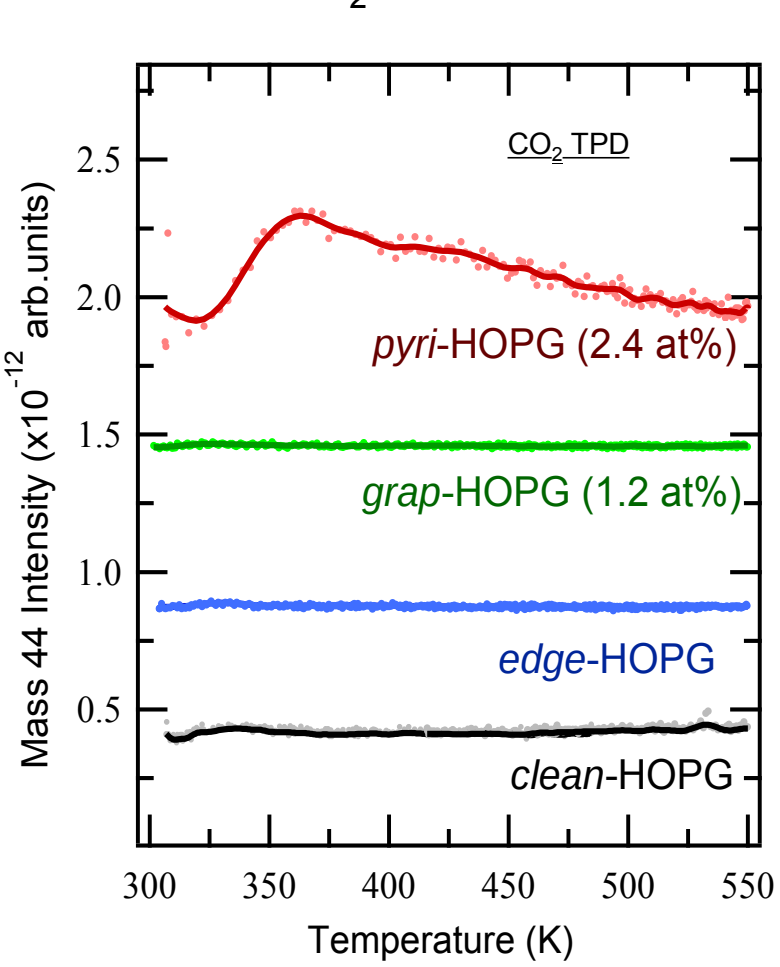

Basic sites are created on pyridinic N-HOPG

ORR activity of HOPG model catalysts

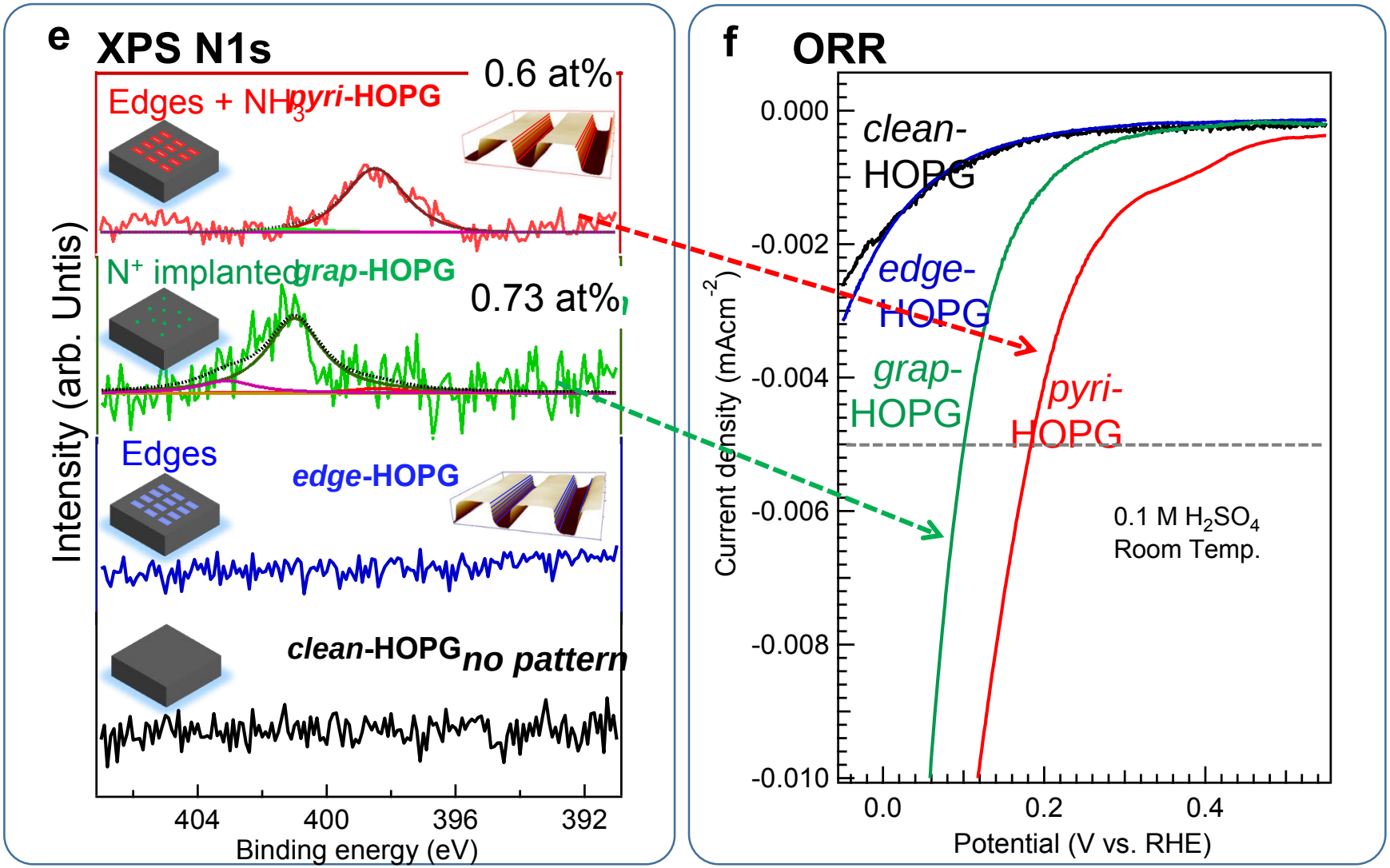

High catalytic activity for pyridinic N-HOPG

ORR current density of N-HOPG model depends on Pyridinic N in 1st order.

ORR of different N-HOPG with different N concentratio

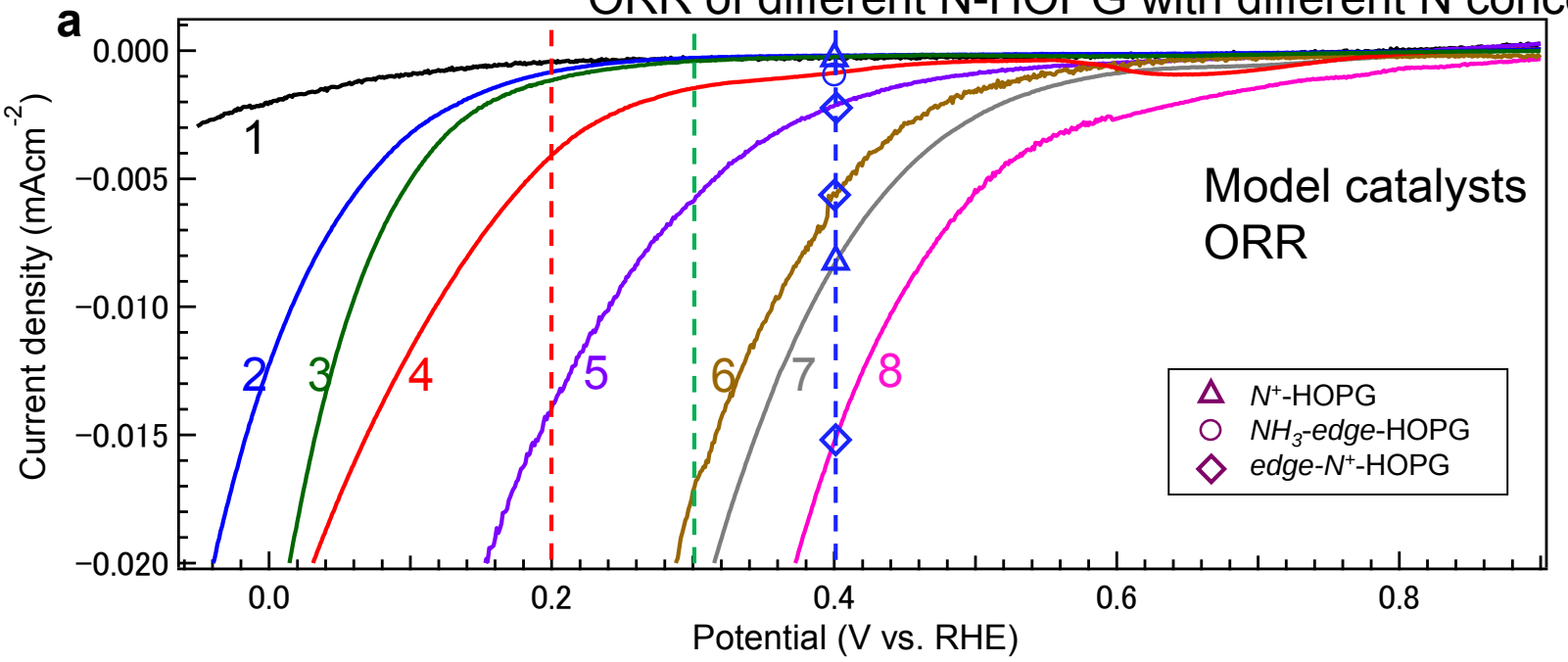

j at different V with pyridinic N concentration Onset potential with pyridinic N concentratio

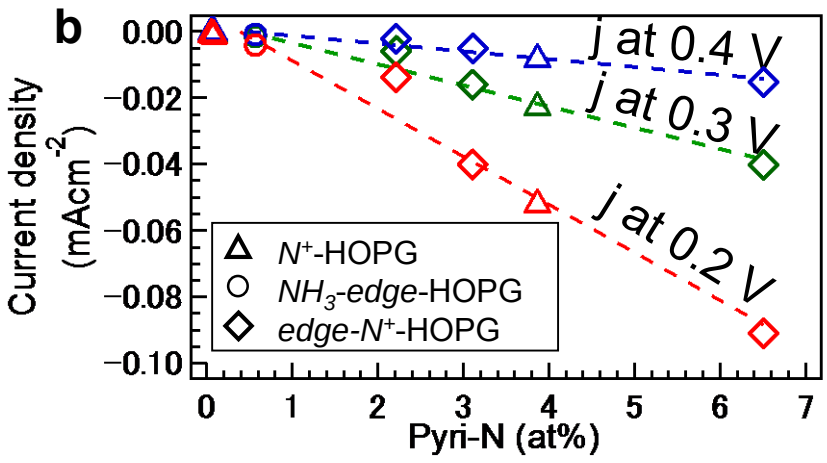

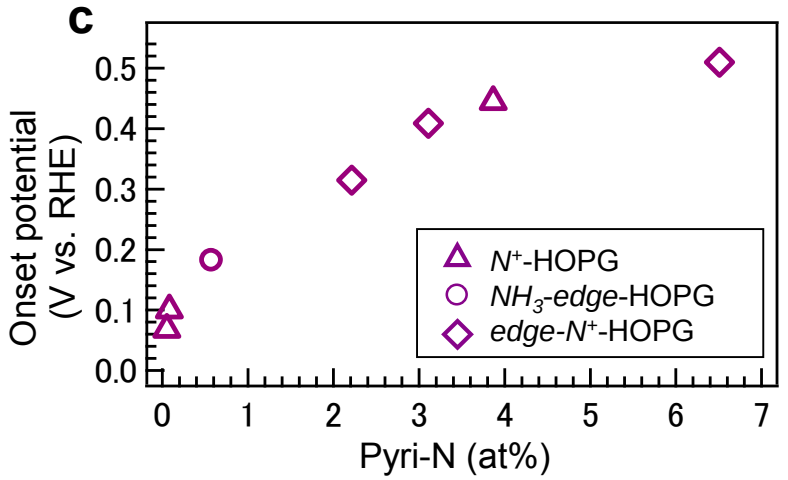

Further indicates that active site is created by pyridinic N!

ORR mechanism on nitrogen doped carbon materials

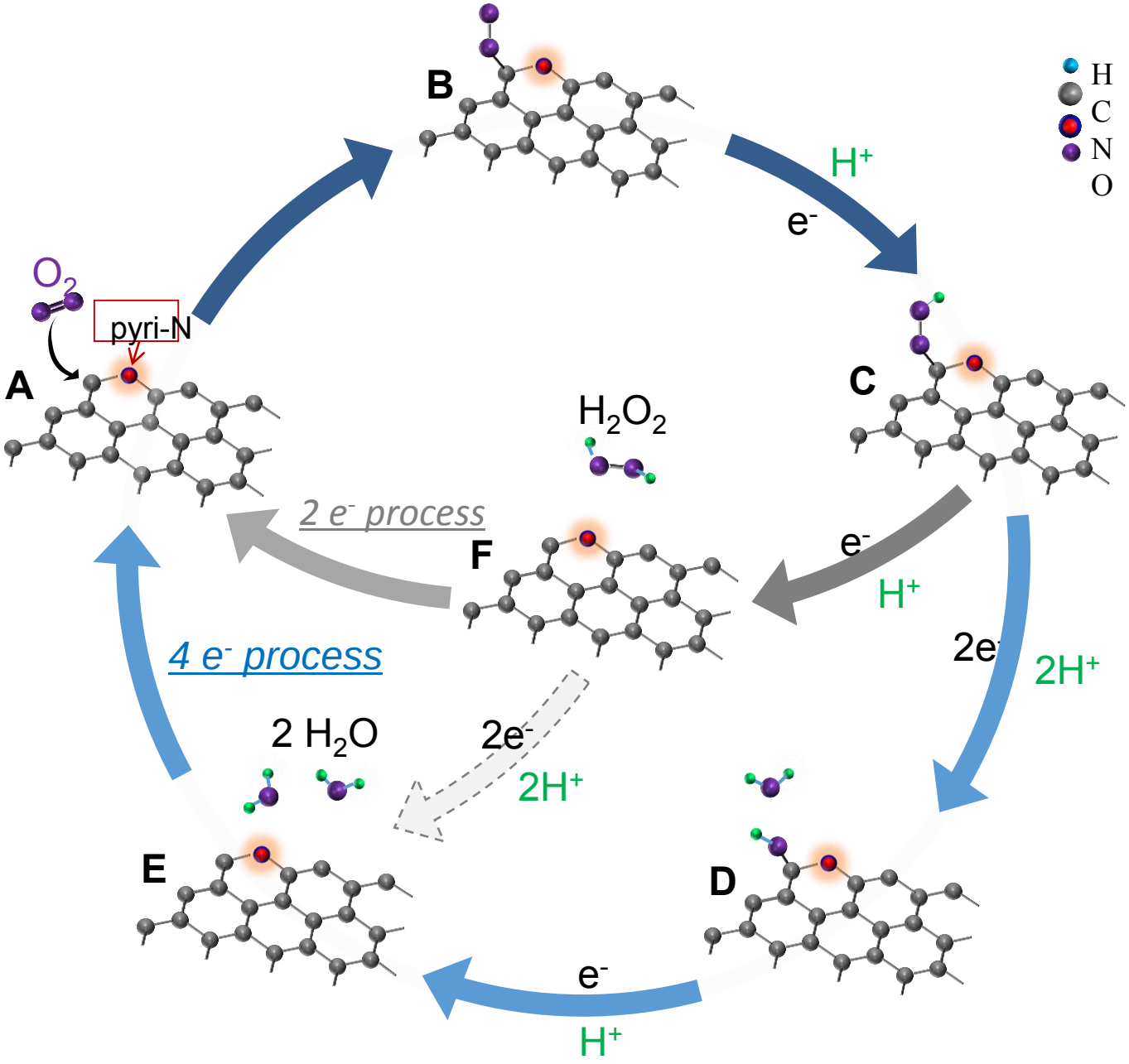

Non-bonding state & acid/base properties

Why pyridinic nitrogen?

Pyridinic nitrogen creates basic sites?

Where are acid/base sites in graphitic materials?

Acid : Accept lone pair

Base : Donate lone pair

Energy levels & band structure for π conjugative system

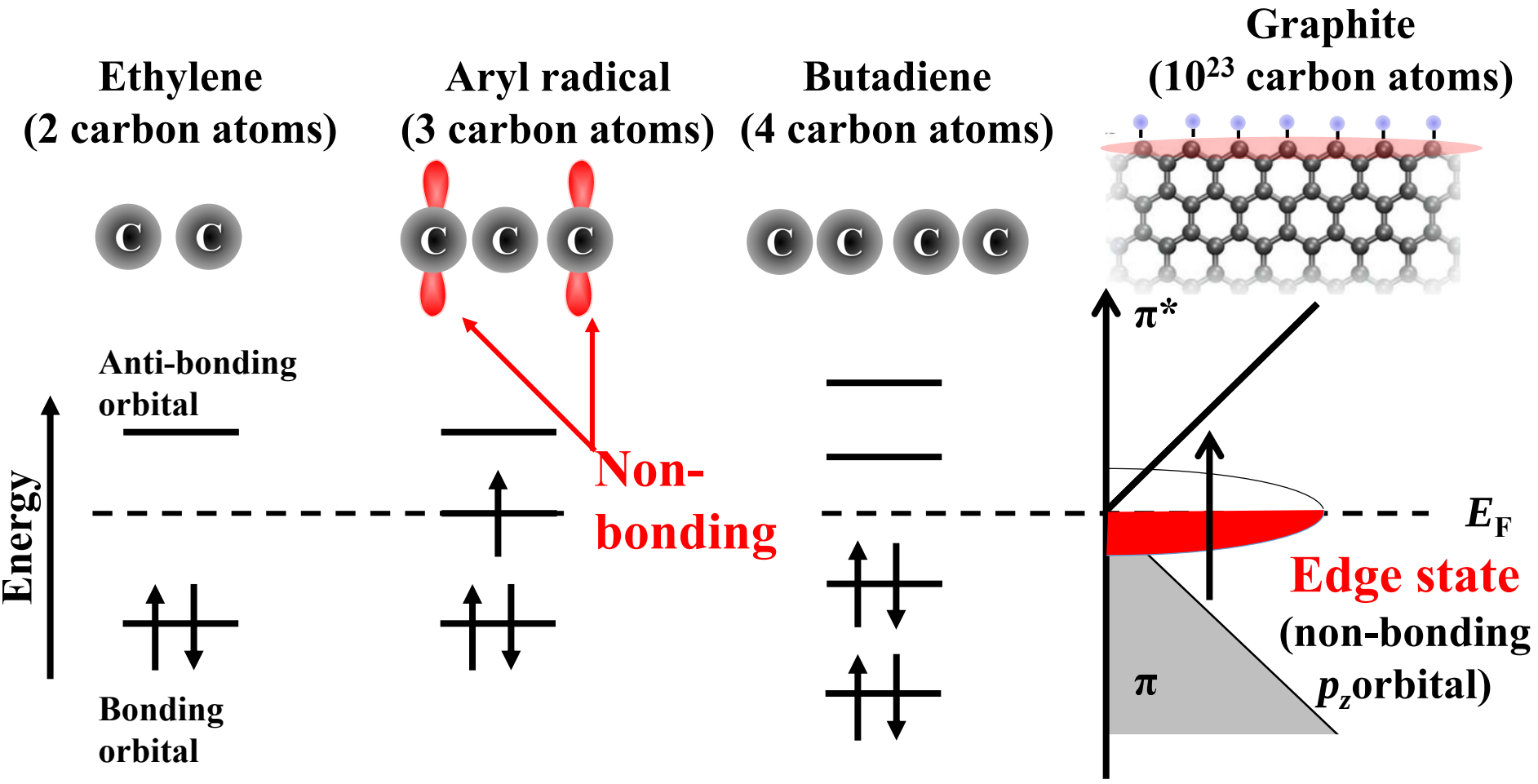

Edge states are equivalent with non-bonding states

Electronic structure of zigzag edge

Graphite

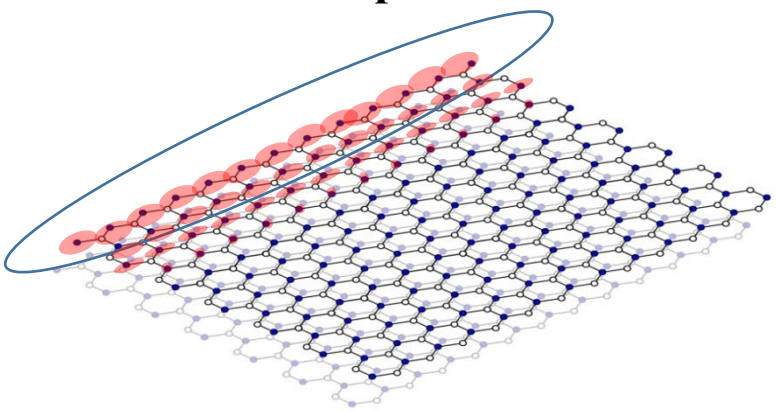

Localized pz electronic states (Edge states)

Zigzag edge

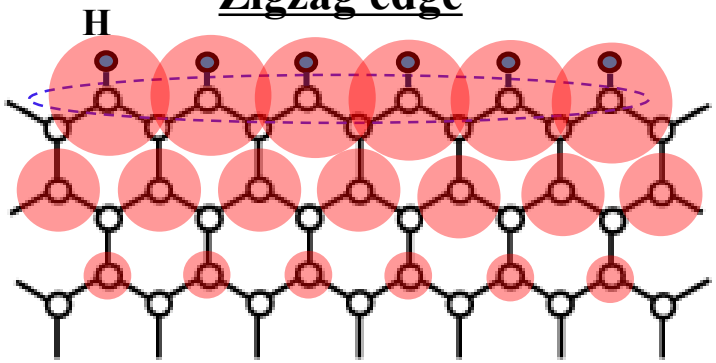

Mitsutaka Fujita, et al, J. Phys.Soc. Japan **65**, 1920 (1996).

Y. Kobayashi, et al., Phys. Rev. B **71**, 193406 (2005).

Zigzag edge
DOS

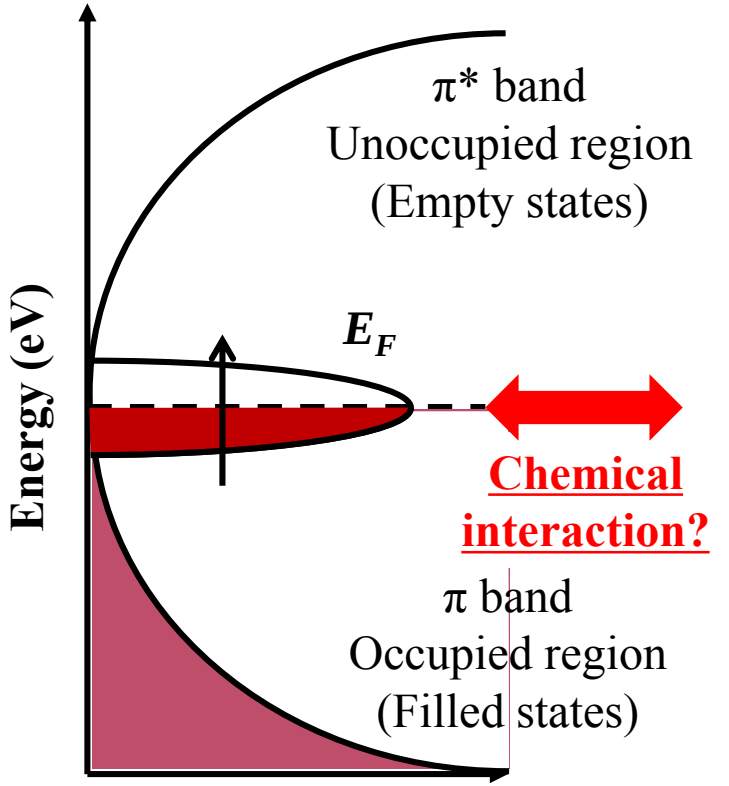

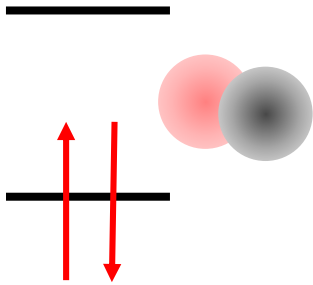

Edge state may be responsible for chemical reactivity of graphitic materials

Electronic structure of zigzag edge

Nitrogen doped graphite

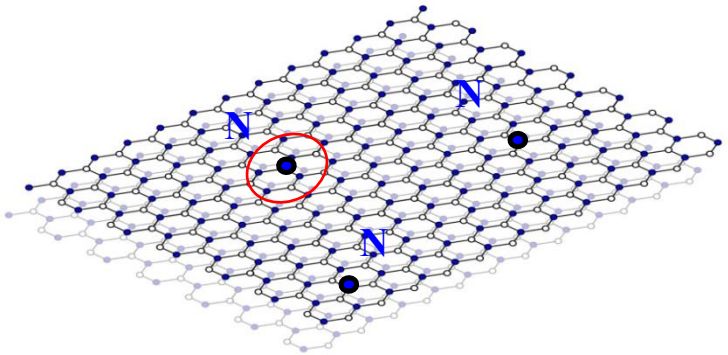

Localized pz electronic states (Edge states)

Near doped nitrogen

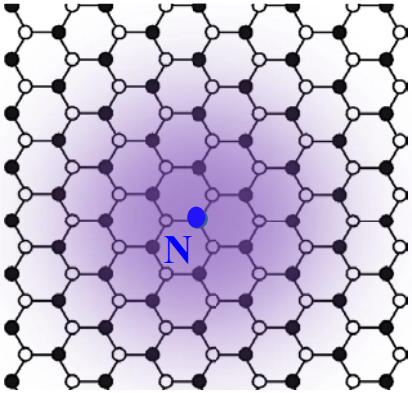

Graphite density of states

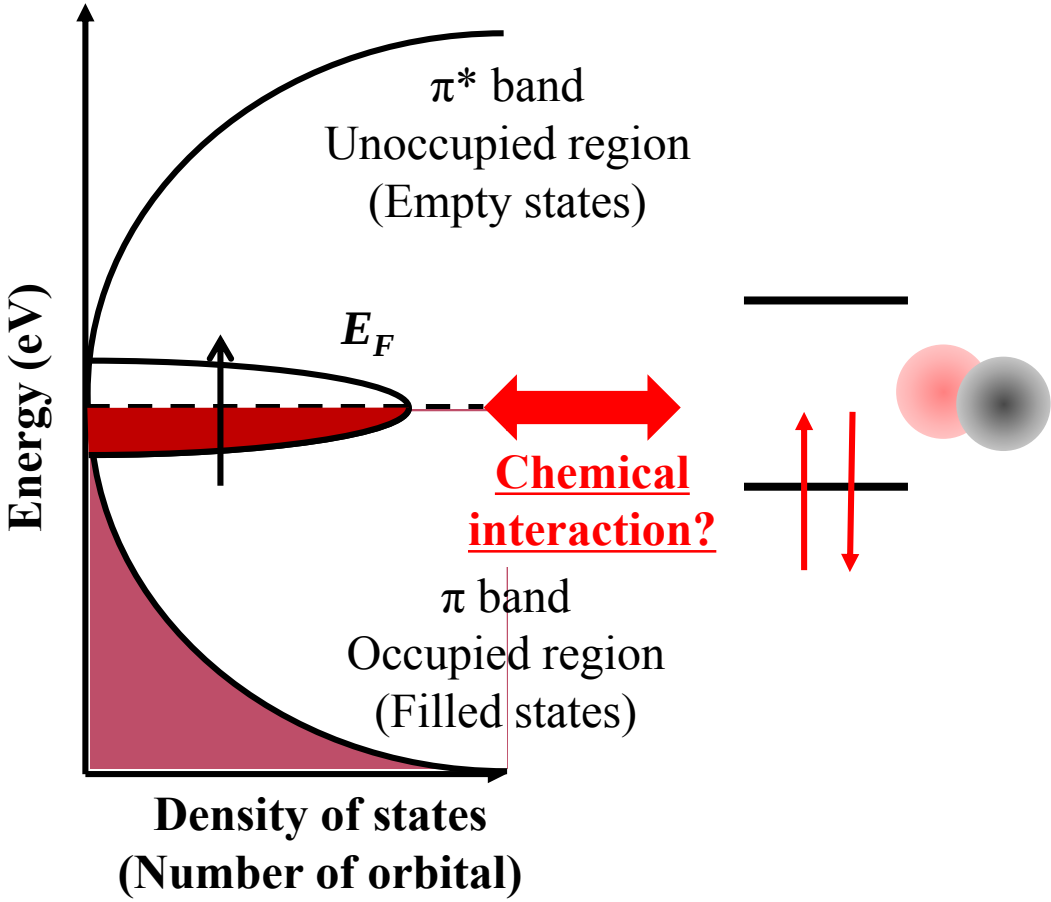

Localized states appear at carbon near doped nitrogen

T. Kondo J. Nakamura et al., Phys. Rev. B **86** (2012) 035436

Graphitic nitrogen

Positively charged

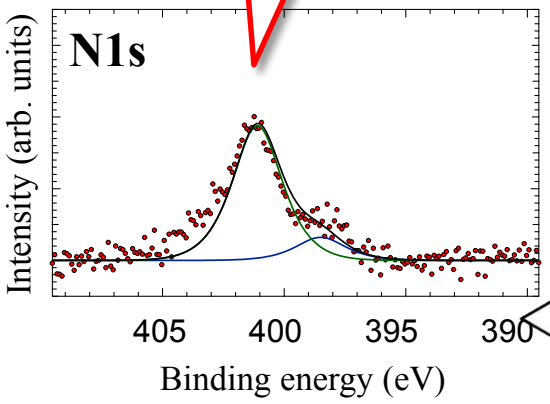

Negatively charged carbon

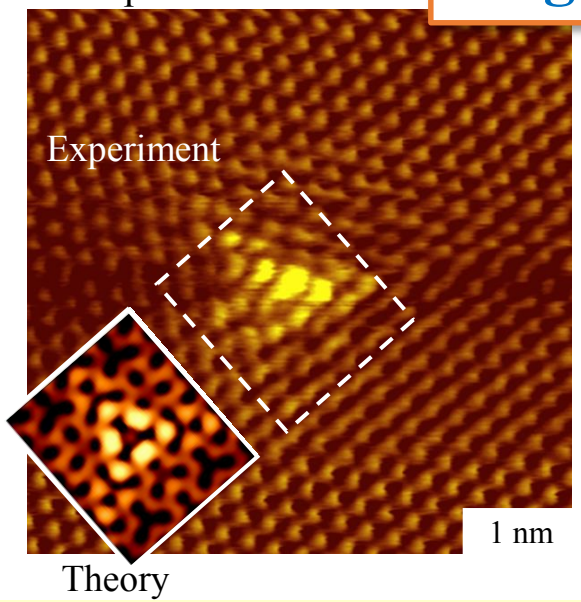

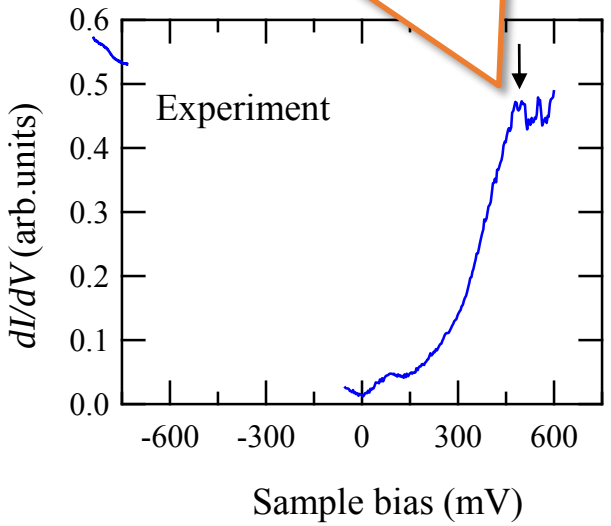

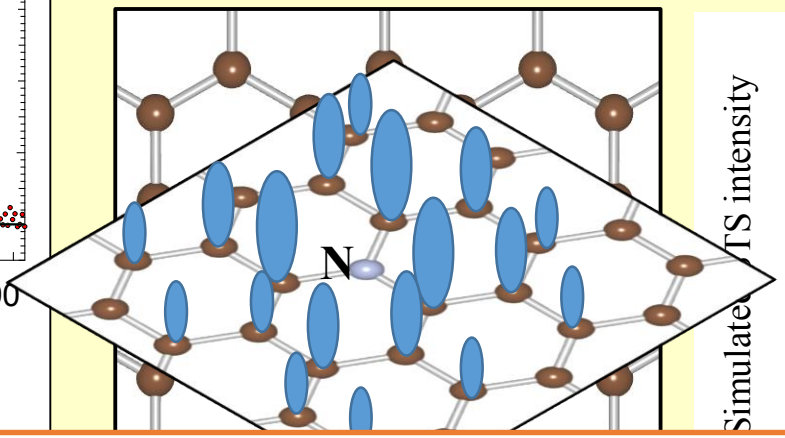

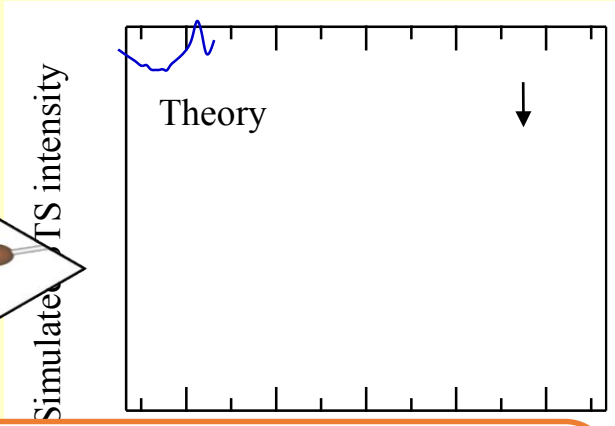

Carbon atoms around graphitic nitrogen may act as Lewis acid

Pyridinic nitrogen

Negatively charged

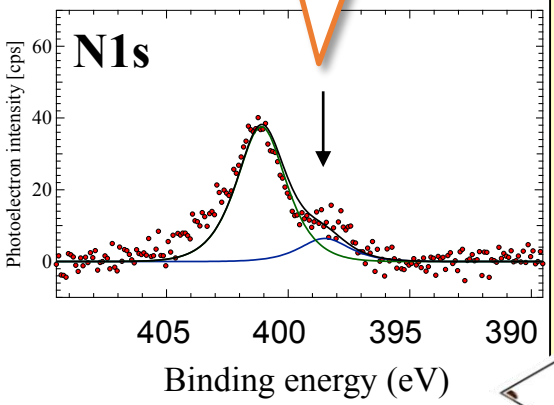

Positively charged carbon

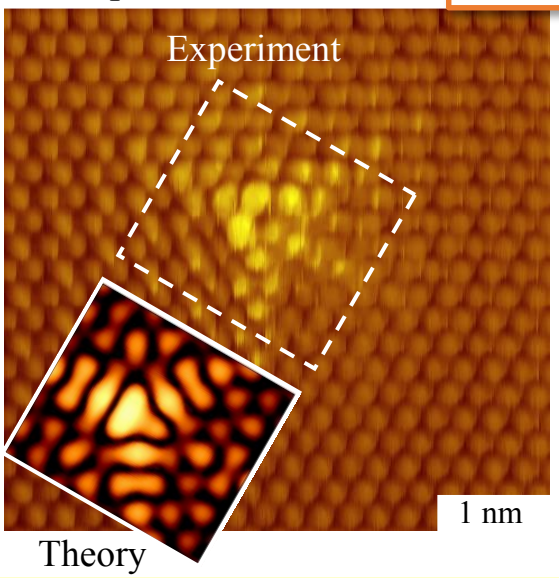

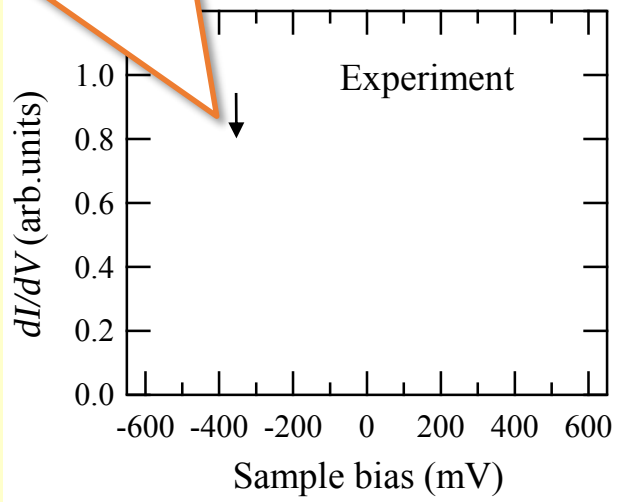

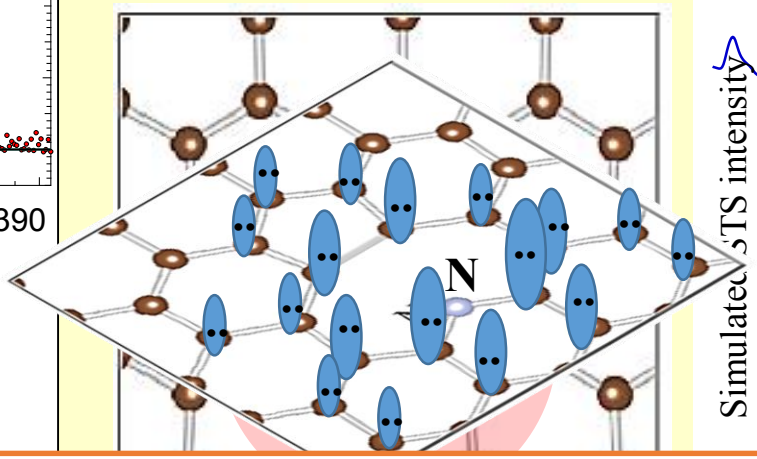

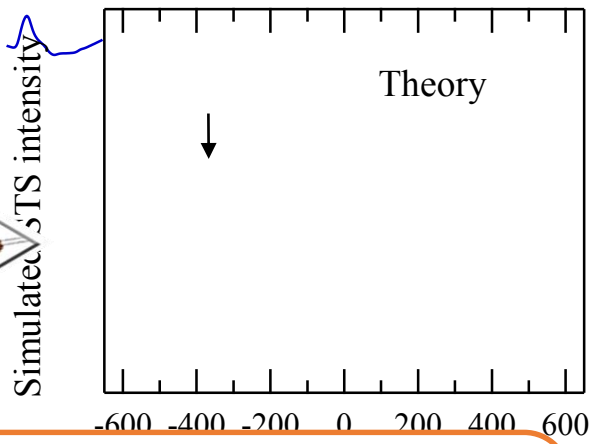

Carbon atoms around pyridinic nitrogen may act as Lewis base

Conclusions

1. Pyridinic-N creates active sites of ORR at which O_2 adsorption may take place as the initial step of ORR.

2. Pyridinic-N creates basic sites.

3. Acid/base properties are originated from non-bonding states.

4. The non-bonding state becomes occupied or unoccupied state depending on the charge of carbon.